始

電氣試驗所研究報告

第二百三十五號

RESEARCHES
OF THE
ELECTROTECHNICAL LABORATORY

KIYOSHI TAKATSU, DIRECTOR.

NO. 235

STUDY ON THE DESIGN OF INDUCTION WATTHOUR METER

By

Seikichi JIMBO

August, 1928.

ELECTROTECHNICAL LABORATORY,
MINISTRY OF COMMUNICATIONS,
TOKYO, JAPAN.

RESEARCHES
OF THE
ELECTROTECHNICAL LABORATORY

KIYOSHI TAKATSU, DIRECTOR.

NO. 235

STUDY ON THE DESIGN OF INDUCTION WATTHOUR METER

By

Seikichi JIMBO

SYNOPSIS

In this paper, it has been intended to offer the materials for the design of the induction watthour meter.

In the first two chapters, the driving torque and the retarding torque have been investigated theoretically, supposing that the magnetic flux are uniformly distributed within the boundary circles. The author has proposed the geometrical constants which have the important meanings for the design and the criticism of the meter. General principles on these constants have been established which will be available to simplifying the calculation of the torque. This constant for the driving torque where the boundary circles intersect mutually has been deduced. It has been illustrated how these constants depend on the relative dimensions of boundary circle with respect to the disc and that the reasonable value of these constants depends merely on the ratio of the radius of boundary circle to that of

the disc. The geometrical constant for the brake magnet has been deduced approximately.

In the second two chapters, the driving torque and the retarding torque have been investigated experimentally. It has been cleared up that the experimental results are in good agreement with the theoretical results about a meter especially made. Various finished meters have been criticized according to the geometrical constant and the configuration of flux distribution, which are obtained experimentally, and the methods of improving these constants have been pointed out. The frictional torques have been measured on various kinds of bearings, in order to resolve the relation between this torque and the weight of the rotating part, and it has been pointed out that the semi-ball pivot bearing will be recommended.

In the third two chapters, the load character and the temperature character have been investigated. The complete equations of these characters have been established and these characters have been analized experimentally. The methods of improving these characters have been explained. The relations between the temperature coefficient of permanent magnet and the ratio of its air gap to its length have been cleared up experimentally.

In the final chapter, the characteristic constants have been proposed which are closely connected with the intrinsic character and the durability of accuracy, and the principal course of design standing on these constants has been presented with many valuable data. A numerical example where the magnetic flux are uniformly distributed within the boundary circle, has been shown.

CONTENTS

TABLE OF SYMBOLS

B . . . . . Flux Density
C . . . . . Characteristic Constant
D . . . . . d/dt
E . . . . . Electromotive Force
G . . . . . Geometrical Constant
I . . . . . Current
K . . . . . Constant
L . . . . . Inductance (Self)
M . . . . . Inductance (Mutual)
P . . . . . Constant
Q . . . . . Constant
R . . . . . Radius of Disc, Resistance
S . . . . . Boundary Area of Flux Distribution
V . . . . . Voltage Drop
W . . . . . Weight of Moving Part
W_i . . . . . Watt Loss in Pressure Coil
Z . . . . . Impedance
AT . . . . . Ampere Turns in Current Coil
Φ . . . . . Magnetic Flux (Max. Value)
Ψ . . . . . Torque in Mean Value (Given in CM-GR Especially)
Δ_f . . . . . Percentage Variation in Frequency
a . . . . . Radius of Circle
b . . . . . Distance between Two Circles
c . . . . . Thickness of Disc
d . . . . . Distance of Centre of Circle from Rotating Axis
f . . . . . Frequency
f_a . . . . . Angular Velocity of Disc

g . . . . . Gravitational Constant
i . . . . . Current Density
k . . . . . Constant
l . . . . . Constant
m . . . . . Specific Gravity of Disc
n . . . . . Number of Revolution of Disc
p . . . . . I/I_f
q . . . . . Φ_{pl}/Φ_{pm}
r . . . . . Distance, Resistance
r_m . . . . . Mean Resistance per Turn of Pressure Coil
t . . . . . Time
u . . . . . r/a
v . . . . . a/r, Constant
α . . . . . Moment of Inertia, Angle, Coefficient
β . . . . . Damping Coefficient, Angle, Coefficient
γ . . . . . Frictional Torque
δ . . . . . Damping Factor, Length of Air Gap
ε . . . . . Error
θ . . . . . Angle
λ . . . . . Perpendicular Distance
ρ . . . . . Distance, Resistance
σ . . . . . Conductivity of Disc
ω . . . . . $2\pi f$
ϕ . . . . . Angle
ψ . . . . . Angle
ξ . . . . . b/R
η . . . . . d/R
ζ . . . . . a/R
x . . . . . b/a

STUDY ON THE DESIGN OF INDUCTION WATTHOUR METER

By

Seikichi JIMBO

CHAPTER I. INTRODUCTION.

There are many literatures on the induction watthour meter, while any data pertaining to the design of meter have not been found. In this paper, it is intended to offer the materials for the design of meter. Some parts in this researches have been already published,[4][6][17][25] and it has just completed in this paper.

In the chapter II and III, various torques are theoretically studied from some assumptions. In the chapter IV and V, these torques are experimentally studied. In the chaper VI and VII, the load character and temperature character are analytically studied. In the last chapter, the principle of design standing on the characteristic constants is explained. The author thinks that the results presented in this paper will be available as a compass for the design as well as the improvement of meter.

In this paper, the deduction to be easily obtained is omitted, and the term of circle which denotes the boundary circle, in which the flux are uniformly distributed, is frequently used. All quantities in this paper are expressed in c.g.s. units excepting the torque which is especially given in cm-gr.

CHAPTER II. THEORETICAL STUDY ON DRIVING TORQUE.

1. Introduction.

The author now proposes the geometrical constant which will be of important meaning on the design as well as the criticism of the meter, and the theoretical study on the torque is nothing but that on this constant. Any researches on this problem presented hitherto stand on some assumptions. The author thinks that it will be impossible to solve this problem, unless any assumptions, which are as nearly actual state as possible, are supposed. Prof. Rogowsky's works,[1][2] applied the principle of inversion, will be splendid to simplifying the solution. A complete solution has been already obtained by Prof. Otake and Kato,[3][8] applying logarithmic potential, while it will be regreted that the case where the circles intersect is not concerned.

In this paper, the author has been obtained a complete solution derived by the other method, applying the principle of inversion. The results in the case where the circles do not intersect coincide that[1][3][8] presented already, hence in this point there are not any noticeable results, however the following points will be noteworthy:

(1) The geometrical constant is generally represented by the ratio of the perpendicular distance from the rotating axis to the line through two centres to the distance between these centres, considering the centres and the inversions of these centres.

(2) The solution in the case where the circles intersect can be obtained. The first point will be valuable to simplifying the calculation of torque, and the second point will be indispensable to the practicable result.

In this paper, the following assumptions are supposed:

The magnetic flux are uniformly distributed within a circle and the phase angles of magnetic flux are constant everywhere in this circle.

2. General Principles on Geometrical Constant.

We now consider an infinite plane sheet of homogeneous conductor whose conductivity is σ, and the alternating magnetic flux Φ within a boundary area on the sheet is perpendicular to the sheet. In this case, the current density i at any point can be obtained by solving the following equations,

$$\frac{\partial r i_r}{\partial r}+\frac{\partial i_\theta}{\partial \theta}=0$$

$$\int i\cos(ids)\,ds=-\sigma\frac{\partial \Phi}{\partial t} \quad \cdots\cdots\cdots\cdots\cdots\cdots (1)$$

where the line integral must be performed around a closed circuit which does not intersect with the boundary of flux distribution, and ds denotes the elementary length along the circuit. When the boundary of flux distribution is infinitesimal small, the stream line of current is obviously circle, and we have

$$i=-j\frac{\sigma f}{r}\Phi \quad \cdots\cdots\cdots\cdots\cdots\cdots\cdots\cdots (2)$$

where r is the distance between the flux and any considered point. Considering that the magnetic flux is positive, when the direction of flux is from the upper side to the sheet, the direction of current is always in the right angle to the line r measured clockwise around the considered point.

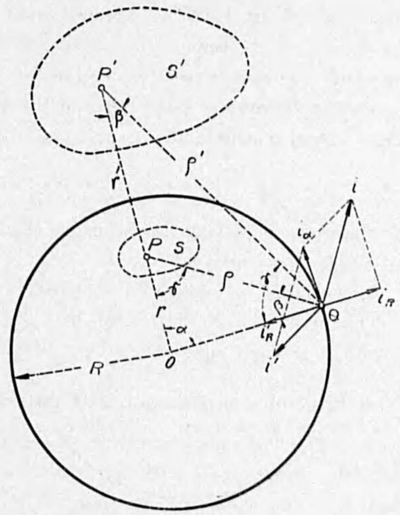

FIG. 1A

Even if the flux are uniformly distributed in a circle, the stream line is also circle and the current density at any point outside of the circle can be similarly found, considering that the total flux concentrate at the centre of circle.

When the sheet is a circle as shown is Fig. 1_A, where the flux concentrate at a point P, the current density can be readily obtained, considering the inversion of P with respect to the circular sheet or the disc. In this case, the radial component of current density i_R must be zero at the circumference of disc. Let the radial component at a point Q due to Φ at P and that due to $-\Phi$ at the inversion of P be i_R, i_R' respectively, then we have

$$\boldsymbol{i}_R = -j\frac{\sigma f}{\rho}\sin\beta\cdot\boldsymbol{\Phi} \qquad \boldsymbol{i}_R' = +j\frac{\sigma f}{\rho'}\sin\gamma\cdot\boldsymbol{\Phi}$$

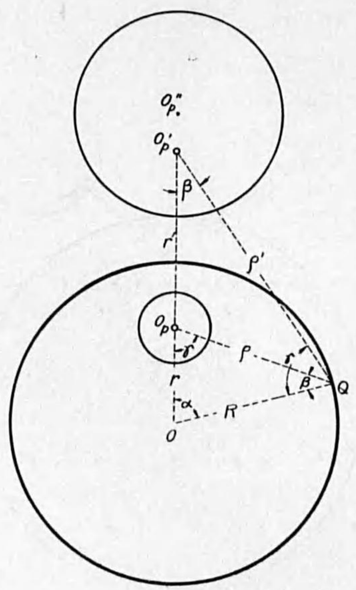

Fig. 1_B

While ΔOPQ is similar to $\Delta OQP'$, therefore we have

$$\boldsymbol{i}_R + \boldsymbol{i}_R' = 0$$

Even if the flux are uniformly distributed within a boundary area S, we can similarly obtained the current density considering the inversion of S with respect to the disc.

When the boundary of flux distribution is circle, we have obviously to consider the centre of circle and the inversion of the above centre with respect to the disc.

Commutative Law.

Now we consider a case as shown in Fig. 2, where Φ_p, Φ_q are uniformly distributed in the boundaries S_p, S_q respectively.

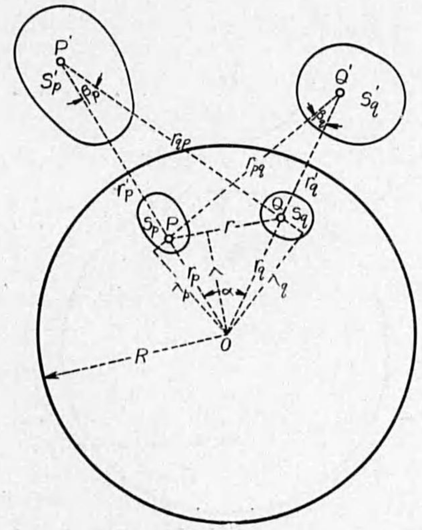

Fig. 2.

Putting

$$\left.\begin{aligned}\boldsymbol{\Phi}_p &= \Phi_p e^{j(\omega t+\psi_p)}\\ \boldsymbol{\Phi}_q &= \Phi_q e^{j(\omega t+\psi_q)}\end{aligned}\right\} \quad \cdots\cdots\cdots\cdots\cdots (3)$$

The current density at the point Q due to the elementary flux $d\boldsymbol{\Phi}_p$ at the point P can be written

$$d\boldsymbol{i}_p = -j\sigma f\left(\frac{1}{r}-\frac{1}{r_{qp}}\right)\cdot d\boldsymbol{\Phi}_p$$

The elementary torque due to $d\boldsymbol{i}_p$ and the elementary flux $d\boldsymbol{\Phi}_q$ can be given by

$$dT_{dpq} = \frac{\sigma c f}{2g}\Phi_p\Phi_q \sin(\psi_p-\psi_q)\cdot\left(\frac{\lambda}{r}-\frac{\lambda_q}{r_{qp}}\right)\cdot\frac{dS_p\,dS_q}{S_p\,S_q}$$

Then the torque T_{dpq} due to Φ_q and the current induced by Φ_p can be written

$$T_{dpq} = \frac{\sigma c f}{2g}\Phi_p\Phi_q \sin(\psi_p-\psi_q)\cdot G_{dpq} \quad \cdots\cdots\cdots (4)$$

G_{dpq} is **Geometrical Constant** proposed by the author and it follows,

$$G_{dpq} = \frac{1}{S_p S_q}\iint_{S_p}\iint_{S_t}\left(\frac{\lambda}{r}-\frac{\lambda_q}{r_{qp}}\right)dS_p\,dS_q \quad \cdots\cdots (5)$$

The direction of torque is counter-clockwise, when its sign is positive.

On the other hand, the torque T_{dqp} due to Φ_p and the current due to Φ_q is similarly obtained.

$$T_{dqp} = -\frac{\sigma c f}{2g}\Phi_p\Phi_q \sin(\psi_q-\psi_p)\cdot G_{dqp} \quad \cdots\cdots\cdots (6)$$

where

$$G_{dqp} = \frac{1}{S_p S_q}\iint_{S_p}\iint_{S_t}\left(\frac{\lambda}{r}-\frac{\lambda_p}{r_{pq}}\right)dS_p\,dS_q \quad \cdots\cdots (7)$$

While $\Delta OP'Q$ is similar to $\Delta OQ'P$, then we have

$$G_{dpq} = G_{dqp}$$

Therefore

$$T_{dpq} = T_{dqp} \quad \cdots\cdots\cdots\cdots\cdots (8)$$

Generally the **Commutative Law** on the driving torque holds, without regard to the boundary of flux distribution.

Geometrical Constant where the Circles do not Intersect.

We will consider here a case as shown in Fig. 3, where the alternating

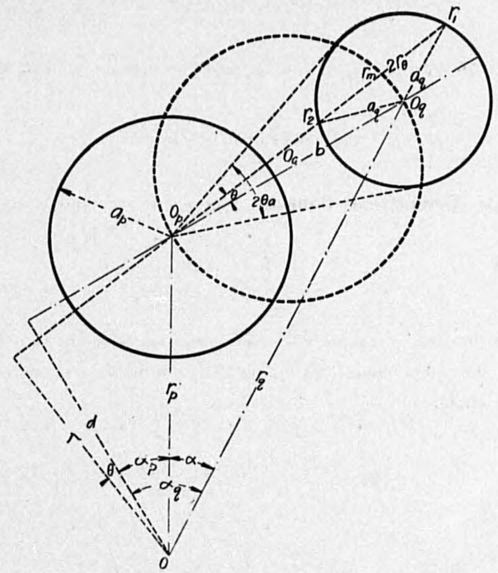

FIG. 3.

magnetic flux are uniformly distributed in two circles on an infinite plane sheet respectively. In this case, the geomerical constant can be represented by

$$G_d=\frac{1}{S_q}\iint_{S_q}\frac{\lambda}{r}\,dS_q \quad \cdots\cdots\cdots\cdots\cdots\cdots (9)$$

or

$$G_d=2\int_{-\theta_a}^{\theta_a}\lambda(r_1-r_2)d\theta\Big/\int_{-\theta_a}^{\theta_a}(r_1^2-r_2^2)d\theta$$

While

$$\lambda=r_p\cos(\alpha_p+\theta)$$

$$d=r_p\cos\alpha_p$$

$$d\cdot\tan\alpha_p=r_p\sin\alpha_p$$

Putting

$$2r_m=r_1+r_2, \qquad 2r_\theta=r_1-r_2$$

Then we have

$$G_d=d\left\{\int_{-\theta_a}^{\theta_a}r_\theta\cos\theta-\tan\alpha_p\int_{-\theta_a}^{\theta_a}r_\theta\sin\theta d\theta\right\}\Big/\int_{-\theta_a}^{\theta_a}r_\theta r_m d\theta$$

While

$$r_\theta=b\sqrt{\cos^2\theta-\cos^2\theta_a}$$

and

$$\int_{-\theta_a}^{\theta_a}r_\theta\sin\theta d\theta=\frac{1}{2}\Big[\cos\theta\sqrt{\cos^2\theta-\cos^2\theta_a}-\cos^2\theta_a\log\left(\cos\theta+\sqrt{\cos^2\theta-\cos^2\theta_a}\right)\Big]_{-\theta_a}^{\theta_a}=0$$

Therefore

$$G_d=d\int_{-\theta_a}^{\theta_a}r_\theta\cos\theta d\theta\Big/\int_{-\theta_a}^{\theta_a}r_\theta r_m d\theta$$

While evidently

$$r_m=b\cos\theta \quad \cdots\cdots\cdots\cdots\cdots\cdots (10)$$

Therefore we have

$$G=d/b \quad \cdots\cdots\cdots\cdots\cdots\cdots (11)$$

The geometrical constant where the circles do not intersect can be generally represented by the ratio of the perpendicular distance from the rotating axis to the line through two centres to the distance between these centres.

The above principle will hold when the boundary of flux distribution is in such manner as to satisfy the relation given by the equation (10).

3. Geometrical Constant where the Circles Intersect.

Now we consider a case as shown in Fig. 4, where two circles intersect. In this case, we must concern two cases, at one case $\pi/4\geqslant\theta\geqslant 0$, or $2\geqslant x\geqslant\sqrt{2}$ and at the other case $\pi/3\geqslant\theta\geqslant\pi/4$, or $\sqrt{2}\geqslant x\geqslant 1$, where $x=b/a$.

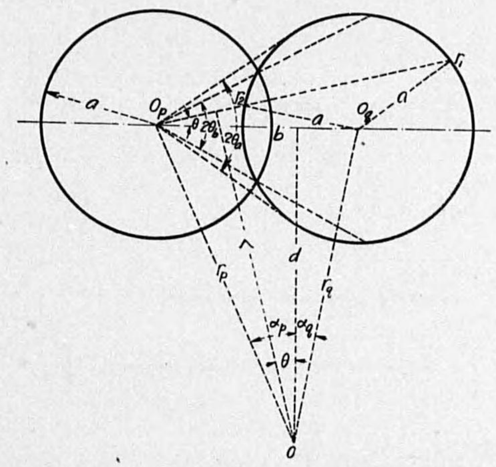

Fig. 4.

At the former case, we have

$$G_d=\frac{d}{\pi a^2}\left\{2\int_{0_b}^{0_a}(r_1-r_2)\cos\theta d\theta+\int_{-0_b}^{0_b}\left(r_1-a+\frac{a^3-r_2^3}{3a^3}\right)\cos\theta d\theta\right\}$$

$$=\frac{d}{\pi a^2}\int_{-0_a}^{0_a}(r_1-r_2)\cos\theta d\theta-\frac{d}{\pi a}\int_{-0_b}^{0_b}\left(\frac{1}{3}\left(\frac{r_2}{a}\right)^3-\frac{r_2}{a}+\frac{2}{3}\right)\cos\theta d\theta$$

where the first term is obviously d/b, then G_d can be written

$$G_d=(1-k_x) \quad \cdots\cdots\cdots\cdots\cdots\cdots \quad (12)$$

where

$$k_x=\frac{x}{\pi}\int_{-0_b}^{0_b}\left(\frac{1}{3}\left(\frac{r_2}{a}\right)^3-\frac{r_2}{a}+\frac{2}{3}\right)\cos\theta d\theta$$

At the latter case, we have

$$G_d=\frac{d}{b}(1-k_x+k_x')$$

where

$$k_x'=\frac{2x}{\pi}\int_{0_b}^{0_a}\left(\frac{r_1}{a}-\frac{r_2}{a}\right)\left(\frac{r_1^2+r_1r_2+r_2^2}{3a^2}-1\right)\cos\theta d\theta$$

While the last term is negligible, so that G_d can be generally expressed by the equations (12).

k_x can be obtained as follows, putting

$$\Delta=\sqrt{1-x^2\sin^2\theta}$$

Then we have

$$\frac{1}{3}\left(\frac{r_2}{a}\right)^3-\frac{r_2}{a}+\frac{2}{3}=\frac{4}{3}x^2\sin^2\theta\Delta+\left(\frac{2}{3}-x^2\right)\Delta$$

$$+\frac{4}{3}x^3\cos^2\theta-x^3\cos\theta+\frac{2}{3}$$

And

$$\int\sin^2\theta\cos\theta\Delta d\theta=\frac{-1}{4x^2}\left\{\Delta^3\sin\theta-\frac{1}{2}\left(\Delta\sin\theta+\frac{1}{x}\sin^{-1}(x\sin\theta)\right)\right\}$$

$$\int\Delta\cos\theta d\theta=\frac{1}{2}\left\{\Delta\sin\theta+\frac{1}{x}\sin^{-1}(x\sin\theta)\right\}$$

$$\int\cos^4\theta d\theta=\frac{3}{8}\left\{\frac{2}{3}\sin\theta\cos^3\theta+\sin\theta\cos\theta+\theta\right\}$$

Therefore

$$k_x=\frac{1}{\pi}\left\{\sin 2\theta_b\left(1+\frac{x^2}{2}\right)-2\theta_b(x^2-1)\right\} \quad \cdots\cdots\cdots \quad (13)$$

where

$$\theta_b=\cos^{-1}x/2$$

Then the term k_x is dependent on x only.

4. Practical Case.

Now we consider the practical case as shown in Fig. 5. Let O_p', O_{q_1}', O_{q_2}' be the inversions of O_p, O_{q_1}, O_{q_2} respectively, then we can immediately obtained the equation of driving torque from the equations (11), (12) and (13).

$$W_d=\frac{2\sigma cf}{g}\Phi_p\Phi_q\sin(\psi_p-\psi_q)G_d \quad \cdots\cdots\cdots \quad (14)$$

putting $\zeta=a/R$, $\xi=b/R$, $\eta=d/R$

Then we have

$$G_d=(1-k_x-k_i) \quad \cdots\cdots\cdots\cdots\cdots \quad (15)$$

where

$$\left.\begin{aligned}k_x&=\frac{1}{\pi}\left\{\sin 2\theta_b\left(1+\frac{x^2}{2}\right)-2\theta_b(x^2-1)\right\} \quad \text{for} \quad x\leqslant 2\\ &=0 \quad\cdots\cdots\cdots\cdots \quad \text{for} \quad x>2\end{aligned}\right\} \quad (16)$$

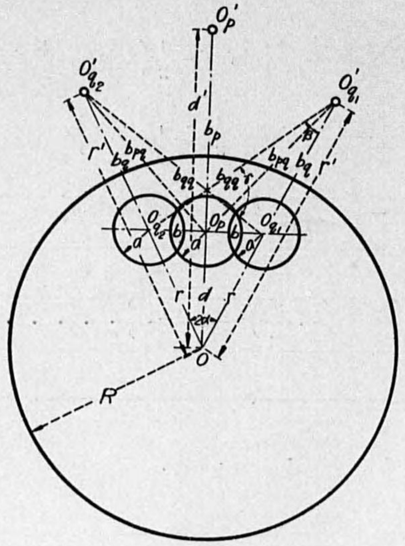

Fig. 5.

$$k_i=\frac{\xi^2}{(1-\eta^2)^2+\xi^2\eta^2} \quad \cdots\cdots\cdots\cdots\cdots\cdots \quad (17)$$

In the design of meter, the geometrical constant must be chosen as large as possible, while this constant depends on ξ, η and ζ, so that it will be important matter to determine these values reasonably.

The relations between G_d and these values are shown in Table I.

The relation between G_d and ξ, where η and ζ are given, is illustrated in Fig. 6 A, and G_d is maximum approximately when

$$\xi=\sqrt{2}\zeta \quad \cdots\cdots\cdots\cdots\cdots\cdots\cdots\cdots \quad (18)$$

The relation between G_d and η, where $\xi=\sqrt{2}\zeta$ is shown in Fig. 6 B, and G_d is maximum when

$$\eta_m=0.9-1.4\zeta \quad \cdots\cdots\cdots\cdots\cdots\cdots\cdots\cdots \quad (19)$$

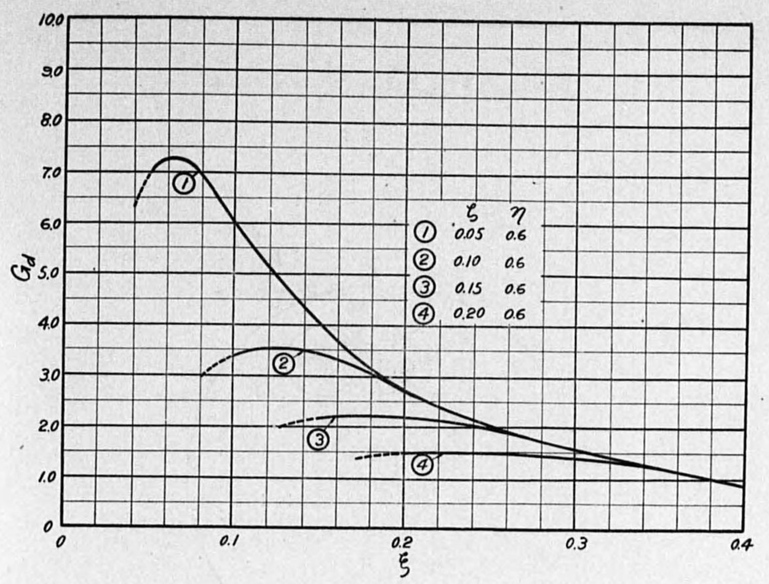

Fig. 6A

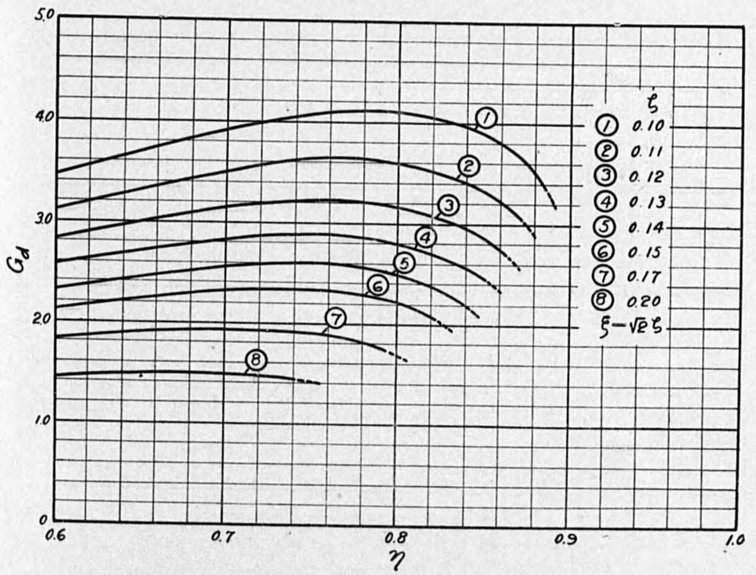

Fig. 6B

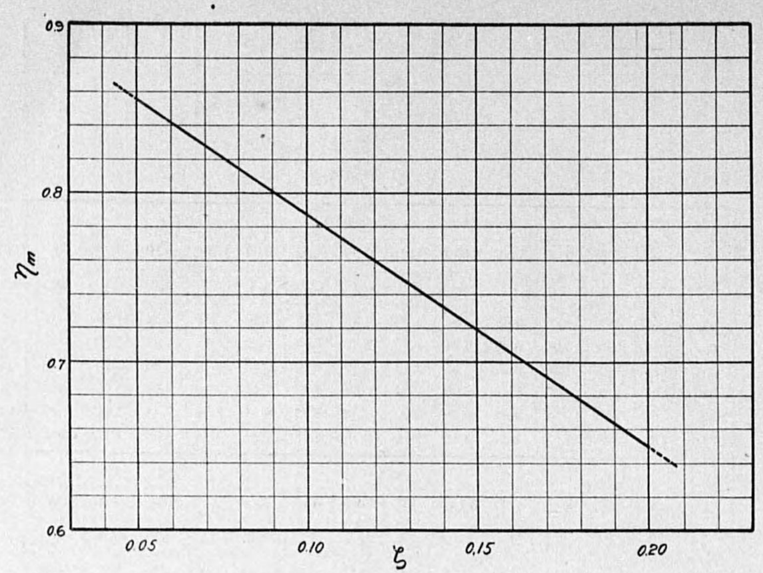

FIG. 6C

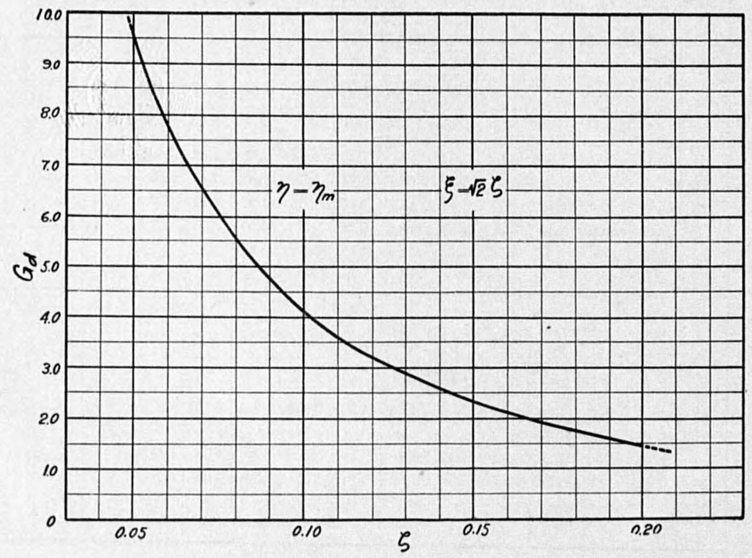

FIG. 6D

TABLE I.

G_d

ζ=0.05														
ξ	0.05	0.055	0.06	0.065	0.0707	0.075	0.08	0.085	0.09	0.095	0.10	0.20	0.30	0.40
η \ $\varkappa$	1.0	1.1	1.2	1.3	1.414	1.5	1.6	1.7	1.8	1.9	2.0	4.0	6.0	8.0
0.4	4.66	4.79	4.86	4.88	4.84	4.78	4.67	4.52	4.35	4.15	3.94	1.89	1.17	0.781
0.5	5.82	5.98	6.06	6.09	6.04	5.96	5.82	5.63	5.42	5.17	4.91	2.33	1.41	0.918
0.6	6.96	7.15	7.25	7.28	7.22	7.13	6.95	6.73	6.46	6.16	5.86	2.72	1.59	0.986
0.7	8.07	8.29	8.40	8.43	8.36	8.24	8.03	7.77	7.46	7.10	6.74	3.00	1.64	0.923
0.8	9.08	9.31	9.42	9.44	9.35	9.20	8.94	8.63	8.26	7.84	7.41	2.97	1.38	0.621
0.9	9.37	9.56	9.62	9.58	9.40	9.19	8.86	8.46	7.99	7.48	6.96	1.87	0.523	—

ζ=0.10														
ξ	0.10	0.11	0.12	0.13	0.1414	0.15	0.16	0.17	0.18	0.19	0.20	0.30	0.40	—
η \ $\varkappa$	1.0	1.1	1.2	1.3	1.414	1.5	1.6	1.7	1.8	1.9	2.0	3.0	4.0	—
0.4	2.29	2.35	2.38	2.38	2.36	2.33	2.27	2.19	2.10	1.99	1.89	1.17	0.781	—
0.5	2.84	2.91	2.95	2.96	2.93	2.88	2.80	2.71	2.59	2.46	2.33	1.41	0.918	—
0.6	3.37	3.46	3.50	3.50	3.46	3.40	3.30	3.18	3.04	2.88	2.72	1.59	0.986	—
0.7	3.84	3.93	3.97	3.96	3.91	3.83	3.71	3.56	3.39	3.20	3.00	1.64	0.923	—
0.8	4.10	4.17	4.20	4.18	4.09	3.99	3.83	3.65	3.44	3.21	2.97	1.38	0.621	—
0.9	—	—	—	—	—	—	—	—	—	—	—	—	—	—

ζ=0.15														
ξ	0.15	0.165	0.18	0.195	0.20	0.2121	0.225	0.24	0.255	0.27	0.285	0.30	0.40	—
η \ $\varkappa$	1.0	1.1	1.2	1.3	1.333	1.414	1.5	1.6	1.7	1.8	1.9	2.0	2.667	—
0.4	1.48	1.51	1.53	1.53	1.53	1.51	1.48	1.44	1.38	1.32	1.24	1.17	0.781	—
0.5	1.82	1.86	1.88	1.88	1.87	1.85	1.81	1.76	1.68	1.60	1.51	1.41	0.918	—
0.6	2.13	2.17	2.19	2.18	2.17	2.14	2.10	2.02	1.93	1.83	1.71	1.59	0.986	—
0.7	2.35	2.39	2.40	2.38	2.37	2.32	2.26	2.17	2.05	1.93	1.79	1.64	0.923	—
0.8	2.29	2.31	2.30	2.26	2.24	2.18	2.11	1.99	1.85	1.71	1.55	—	—	—
0.9	—	—	—	—	—	—	—	—	—	—	—	—	—	—

ζ=0.20														
ξ	0.20	0.22	0.24	0.26	0.2828	0.30	0.32	0.34	0.36	0.38	0.40	—	—	—
η \ $\varkappa$	1.0	1.1	1.2	1.3	1.414	1.5	1.6	1.7	1.8	1.9	2.0	—	—	—
0.4	1.06	1.08	1.10	1.08	1.06	1.04	1.00	0.954	0.901	0.842	0.781	—	—	—
0.5	1.29	1.32	1.32	1.31	1.28	1.25	1.20	1.14	1.07	0.996	0.918	—	—	—
0.6	1.48	1.50	1.50	1.48	1.44	1.40	1.34	1.26	1.18	1.08	0.986	—	—	—
0.7	1.55	1.57	1.56	1.53	1.48	1.42	1.34	1.25	1.14	1.03	—	—	—	—
0.8	—	—	—	—	—	—	—	—	—	—	—	—	—	—
0.9	—	—	—	—	—	—	—	—	—	—	—	—	—	—

Therefore G_d is maximum when $\xi=\sqrt{2}\zeta$, and $\eta=\eta_m$, and in this case we have

$$G_d=0.38/\zeta \quad \cdots\cdots\cdots\cdots\cdots\cdots \quad (20)$$

These results will have important meaning on the design of meter, and the author thinks that in actual case the similar relations shall be established, though it may be somewhat complicate.

CHAPTER III. THEORETICAL STUDY ON RETARDING TORQUE.

1. Introduction.

In this chapter, we will consider of the electromagnetic retarding torques. There are two kinds of torques, one of them is the torque due to the alternating magnetic flux and the other is that due to the brake magnet.

On the former, a complete result has been already performed by Prof. Otake and Kato.[6][8] This torque will not be important such as the driving torque, hence in this paper the approximate solution will be given.

On the latter, there are not any complete results, while the solution will be more complicate. In this paper, the approximate solution, which will be available in practice, can be obtained.

The following points will be noteworthy:

(1) The geometrical constant for single pole can be generally represented by the square of the ratio of the distance from the rotating axis to the centre of circle to the radius of circle.

(2) The geometrical constant for the interaction between two poles can be generally given by $\frac{r_p r_q}{r^2}\cos(\alpha_p+\alpha_q)$, where r_p and r_q are the distances from the rotating axis to the centres of circles, r the distance between these centres and α_p, α_q the angles between r and r_p, r_q measured in same direction from the line r respectively.

(3) The geometrical constant due to brake magnet can be obtained. The first two points will be available to simplifying the calculation of retarding torque, and the last point will give a important material on the design of brake magnet. The results on the retarding torque in practical case presented in this paper, of course, coincide that obtained already.[5][8]

2. General Principles on Geometrical Constant for Retarding Torque.

Now we consider a case where the magnetic flux are uniformly distributed in a circle on an infinite plane sheet as shown in Fig. 7, and assume that the linear velocity of disc is $2\pi f_d r_p$ everywhere in the circle; in other words, the circle is very small compared with the disc.

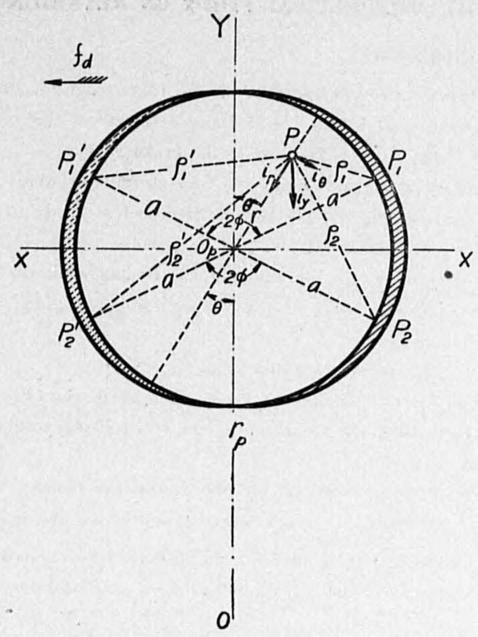

FIG. 7.

The change of flux per second at an elementary length of the circumference $\Delta\Phi_p$ is written

$$\Delta\Phi_p=-\frac{2f_d r_p}{a}\Phi_p\sin\phi\cdot d\phi \quad \cdots\cdots\cdots\cdots \quad (21)$$

where ϕ is measured clockwise from the line r_p around the centre O_p.

Single Pole.

Let the components of induced current be i_r, i_θ respectively, then we have

$$i_r=-\frac{\sigma f_d r_p}{\pi a}\Phi_p\int_0^{\frac{\pi}{2}}\left\{\frac{\sin\psi_1}{\rho_1}+\frac{\sin\psi_2}{\rho_2}+\frac{\sin\psi_1'}{\rho_1'}+\frac{\sin\psi_2'}{\rho_2'}\right\}\sin\phi d\phi$$

where $\psi_1=\angle P_1PO_p$, $\psi_2=\angle P_2PO_p$, $\psi_1'=\angle P_1'PO_p$, $\psi_2'=\angle P_2'PO_p$.
While

$$\rho_1^2=a^2+r^2-2ar\cos(\phi-\theta)$$

$$\rho_2^2=a^2+r^2+2ar\cos(\phi+\theta)$$

$$\rho_1'^2=a^2+r^2-2ar\cos(\phi+\theta)$$

$$\rho_2'^2=a^2+r^2+2ar\cos(\phi-\theta)$$

Now putting $u=r/a$, then $u\leqslant 1$.
Let

$$k=\frac{2u}{1+u^2}\leqslant 1$$

$$k'=\sqrt{1-k^2}=\frac{1-u^2}{1+u^2}\leqslant 1.$$

Then we have

$$i_r=-\frac{2\sigma f_a r_p}{\pi a^2(1+u^2)}\Phi_p\int_0^{\frac{\pi}{2}}\left\{\frac{\sin(\phi-\theta)}{1-k^2\cos^2(\phi-\theta)}+\frac{\sin(\phi+\theta)}{1-k^2\cos^2(\phi+\theta)}\right\}\sin\phi d\phi \quad \cdots\cdots (22)$$

While

$$\int\frac{\sin^2\phi d\phi}{1-k^2\cos^2\phi}=\frac{1}{k^2}\left\{\phi-k'\tan^{-1}\left(\frac{\tan\phi}{k'}\right)\right\}$$

$$\int\frac{\sin\phi\cos\phi d\phi}{1-k^2\cos^2\phi}=\frac{1}{2k^2}\log\left(\cos\phi-\frac{1}{k^2}\right)$$

Therefore

$$\int_0^{\frac{\pi}{2}}\frac{\sin(\phi-\theta)\sin\phi}{1-k^2\cos^2(\phi-\theta)}d\phi=\frac{\pi(1-k')}{2k^2}\cos\theta+\frac{\sin\theta}{2k^2}\log\frac{k^2\sin^2\theta-1}{k^2\cos^2\theta-1}$$

$$\int_0^{\frac{\pi}{2}}\frac{\sin(\phi+\theta)\sin\phi}{1-k^2\cos^2(\phi+\theta)}d\phi=\frac{\pi(1-k')}{2k^2}\cos\theta-\frac{\sin\theta}{2k^2}\log\frac{k^2\sin^2\theta-1}{k^2\cos^2\theta-1}$$

Therefore we have

$$i_r=-\frac{\sigma f_a r_p}{a^2}\Phi_p\cos\theta \quad \cdots\cdots (23)$$

Similarly we have

$$i_\theta=-\frac{\sigma f_a r_p}{\pi a}\Phi_p\int_0^{\frac{\pi}{2}}\left\{\frac{\cos\psi_1}{\rho_1}+\frac{\cos\psi_2}{\rho_2}+\frac{\cos\psi_1'}{\rho_1'}+\frac{\cos\psi_2'}{\rho_2'}\right\}\sin\phi d\phi$$

$$=-\frac{\sigma f_a r_p}{a^2}\Phi_p\sin\theta \quad \cdots\cdots (24)$$

From these results, we have

$$i_x=0 \quad \cdots\cdots (25)$$

$$i_y=-\frac{\sigma f_a r_p}{a^2}\Phi_p \quad \cdots\cdots (25)$$

Now we know that the current densities are constant everywhere in the circle and its direction coincides that of r_p.

Therefore we have

$$\Psi_{bp}=-\frac{\sigma c f_a}{2g}\Phi_p^2 G_{bp} \quad \cdots\cdots (26)$$

where

$$G_{bp}=r_p^2/a^2 \quad \cdots\cdots (27)$$

Interaction Between Two Poles.

In Fig. 8, let the component of current density outside of the circle be i_r, i_θ respectively, then we have

$$i_r=-\frac{\sigma f_a r_p}{\pi}\Phi_p\int_0^{\frac{\pi}{2}}\left\{\frac{\sin(\phi-\theta)}{\rho_1^2}+\frac{\sin(\phi+\theta)}{\rho_2^2}+\frac{\sin(\phi+\theta)}{\rho_1'^2}+\frac{\sin(\phi-\theta)}{\rho_2'^2}\right\}\sin\phi d\phi$$

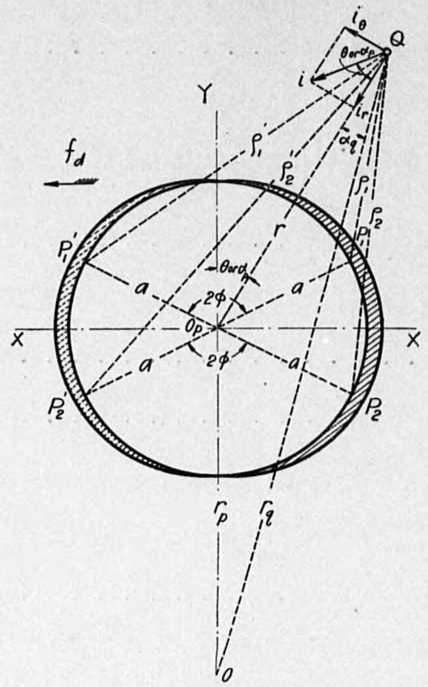

Fig. 8.

Putting $v=a/r$, then $v \leqslant 1$, and let

$$l=\frac{2v}{1+v^2} \leqslant 1$$

$$l'=\sqrt{1-l^2}=\frac{1-v^2}{1+v^2} \leqslant 1$$

Then

$$\rho_1^2=r^2(1+v^2)\,(1-l\cos(\phi-\theta))$$

$$\rho_2^2=r^2(1+v^2)\,(1+l\cos(\phi+\theta))$$

$$\rho_1'^2=r^2(1+v^2)\,(1-l\cos(\phi+\theta))$$

$$\rho_2'^2=r^2(1+v^2)\,(1+l\cos(\phi-\theta))$$

Therefore

$$i_r=-\frac{\sigma f_d r_p}{r^2}\Phi_p\cos\theta$$

Similarly we have

$$i_\theta=-\frac{\sigma f_d r_p}{r^2}\Phi_p\sin\theta$$

Now putting $\theta=\alpha_p$, then we have

$$i_r=-\frac{\sigma f_d r_p}{r^2}\Phi_p\cos\alpha_p \quad \cdots\cdots\cdots\cdots\cdots\cdots \quad (28)$$

$$i_\theta=-\frac{\sigma f_d r_p}{r^2}\Phi_p\sin\alpha_p \quad \cdots\cdots\cdots\cdots\cdots\cdots \quad (29)$$

Therefore

$$i=-\frac{\sigma f_d r_p}{r^2}\Phi_p \quad \cdots\cdots\cdots\cdots\cdots\cdots \quad (30)$$

The current density at any point outside of the circle can be easily obtained by considering the centre of circle and the angle between i and r is always equal to that between r and r_p.

Even if the plane sheet is a circle, the current density at any point on the disc can be obtained by considering the inversion of the centre of circle with respect to the disc. In this case, the radial component of current density on the circumference of the disc must be zero. Now considering on Fig. 1 B, we have.

$$i_R=-\frac{\sigma f_d r}{\rho^2}\cos(\gamma-\beta)\Phi_p$$

$$i_R' = \frac{\sigma f_d r'}{\rho'^2} \cos(\gamma-\beta)\Phi_p$$

While ΔOO_pQ is similar to $\Delta OQO_p'$, then we have

$$i_R + i_R' = 0$$

Now the retarding torque can be easily obtained by the preceding assumption,

$$\Psi_{bpq} = -\frac{\sigma c f_d}{2g}\Phi_p\Phi_q \cos(\psi_p-\psi_q) G_{bpq} \quad \cdots\cdots\cdots (31)$$

where

$$G_{bpq} = -\frac{r_p r_q}{r^2}\cos(\alpha_p+\alpha_q) \quad \cdots\cdots\cdots (32)$$

The geometrical constant for the interaction between two poles can be generally represented by $\frac{r_p r_q}{r^2}\cos(\alpha_p+\alpha_q)$, where r_p and r_q are the distances from the rotating axis to the centres of circles, r the distance between these centres, and α_p, α_q the angles between r and r_p or r_q measured in same direction from the line r respectively.

3. Practical Case.

Now we consider the practical case as shown in Fig. 5. Let Φ_p be the magnetic flux at the middle pole, and Φ_q the magnetic flux at the outside pole.

The retarding torque due to Φ_p is written

$$\Psi_{bp} = -\frac{\sigma c f_d}{2g}\Phi_p^2 G_{bp}, \quad \cdots\cdots\cdots (33)$$

$$G_{bp} = \eta^2\left\{\frac{1}{\zeta^2} - \frac{\eta^2}{(1-\eta^2)^2}\right\} \quad \cdots\cdots\cdots (34)$$

The retarding torque due to Φ_q is given

$$\Psi_{bq} = -\frac{\sigma c f_d}{g}\Phi_q^2 G_{bq} \quad \cdots\cdots\cdots (35)$$

$$G_{bq} = (\xi^2+\eta^2)\left(\frac{1}{\zeta^2}+\frac{1}{4\xi^2}\right) - (\xi^2+\eta^2)^3\left\{\frac{1}{(1-(\xi^2+\eta^2))^2} + \frac{\cos\gamma}{(\xi^2+\eta^2)^4 - 2(\eta^2-\xi^2)+1}\right\} \quad \cdots\cdots (36)$$

The numerical relations between G_{bp} or G_{bq} and ξ, η, ζ are shown in Table II. The relation between G_{bp} and η is shown in Fig. 9 A. When $\eta=\eta_m$, the relation between G_{bp} and ζ can be written

$$G_{bp} = 0.55/\zeta^2 \quad \cdots\cdots\cdots (37)$$

The relation between G_{bq} and ξ is given in Fig. 9 C, and that between G_{bq} and η when $\xi=\sqrt{2}\zeta$ is shown in Fig. 9 D. When $\xi=\sqrt{2}\zeta$ and $\eta=\eta_m$, we have

$$G_{bq} = 0.65/\zeta^2 \quad \cdots\cdots\cdots (38)$$

Now we consider the characteristic constant C_p, C_q which are closely related with the load character or the voltage character.

Putting

$$C_p = \Psi_{bp}/\Psi_d \quad \cdots\cdots\cdots (39)$$

$$C_q = \Psi_{bq}/\Psi_d \quad \cdots\cdots\cdots (40)$$

From the above equations, it follows,

$$C_p = k_p\frac{f_d}{f}\cdot\frac{\Phi_p}{\Phi_q} \quad \cdots\cdots\cdots (41)$$

$$C_q = k_q\frac{f_d}{f}\cdot\frac{\Phi_q}{\Phi_p} \quad \cdots\cdots\cdots (42)$$

where

$$k_p = G_{bp}/4G_d \quad \cdots\cdots\cdots (43)$$

$$k_q = G_{bq}/2G_d \quad \cdots\cdots\cdots (44)$$

When $\xi=\sqrt{2}\zeta$, and $\eta=\eta_m$, we have

$$k_p = 0.36/\zeta \quad \cdots\cdots\cdots (45)$$

$$k_g=0.85/\zeta \quad \cdots\cdots\cdots\cdots\cdots\cdots \quad (46)$$

These values have the important meaning on the design of meter.

4. Geometrical Constant for Braking Torque.

Now we consider of single magnet as shown in Fig. 10. We assume that the magnetic flux are uniformly distributed in a rectangular boundary and the linear velocity of the disc is constant everywhere in this boundary.

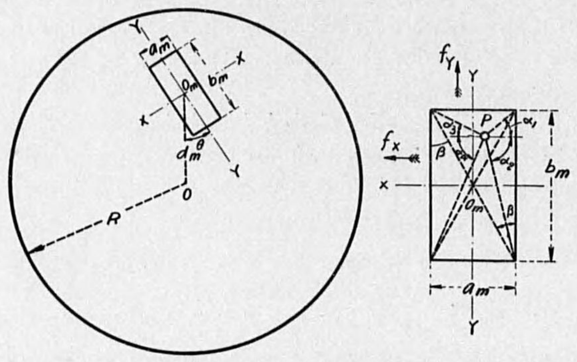

Fig. 10.

Let the component velocities be f_x, f_y, then we have

$$\left.\begin{aligned} f_x&=f_d\cos\theta \\ f_y&=f_d\sin\theta \end{aligned}\right\} \quad \cdots\cdots\cdots\cdots\cdots\cdots \quad (47)$$

The flux change per second at the elementary length of the circumference of the boundary can be written

$$\left.\begin{aligned} \Delta\Phi_x&=-2\pi f_y\frac{d_m}{S_m}\Phi_m dx \\ \Delta\Phi_y&=-2\pi f_x\frac{d_m}{S_m}\Phi_m dy \end{aligned}\right\} \quad \cdots\cdots\cdots\cdots\cdots\cdots \quad (48)$$

where S_m is the area of boundary.

Let the components of current densities in the boundary be i_x, i_y, then i_y due to $\Delta\Phi_x$ and i_x due to $\Delta\Phi_y$ are very small, then we have

$$\left.\begin{aligned} i_x&=-\sigma f_d\frac{d_m}{S_m}\Phi_m\left\{2\pi-(\alpha_1+\alpha_2+\alpha_3+\alpha_4)\right\}\sin\theta \\ i_y&=-\sigma f_d\frac{d_m}{S_m}\Phi_m(\alpha_1+\alpha_2+\alpha_3+\alpha_4)\cos\theta \end{aligned}\right\} \quad \cdots \quad (49)$$

where $(\alpha_1+\alpha_2+\alpha_3+\alpha_4)$ is a function of x and y. Now let its mean value within the boundary be α_m, then it follows

$$\alpha_m=\frac{1}{S_m}\int_{-a_m}^{a_m}\int_{-b_m}^{b_m}\tan^{-1}\frac{b+y}{a+x}\cdot dxdy$$

$$=2\pi-4\tan^{-1}\left(\frac{a_m}{b_m}\right)+\left(1-\frac{a_m}{b_m}\right)\left\{1+\frac{b_m}{a_m}\log\left(1+\frac{a_m^2}{b_m^2}\right)\right\}$$

Putting $\beta=\tan^{-1}a_m/b_m$, then β is very small quantity ($\leqslant 1/3$) in our case, then approximately $\alpha_m=(2\pi+1)-6\beta$, while this value will a good approximation to $(2\pi-4\beta)$. Therefore we can suppose that the current densities are constant in the boundary and the value is the current density at the centre of boundary, i_{x0} and i_{y0}.

And we have

$$\left.\begin{aligned} i_{x0} &= -4\sigma f_{it}\frac{d_m}{S_m}\beta\Phi_m\sin\theta \\ i_{y0} &= -4\sigma f_{it}\frac{d_m}{S_m}\left(\frac{\pi}{2}-\beta\right)\Phi_m\cos\theta \end{aligned}\right\} \quad \cdots\cdots\cdots (50)$$

Neglecting the effect of the inversion, we have

$$\Psi_m = -\frac{2\sigma c f_{it}}{g}\Phi_m^2 G_m \quad \cdots\cdots\cdots\cdots\cdots (51)$$

where

$$G_m = \frac{d_m^2}{S_m}\left(\frac{\pi}{2}+\cos 2\theta\cdot\left(\frac{\pi}{2}-2\beta\right)\right) \quad \cdots\cdots\cdots (52)$$

The relation between G_m and β is shown in Fig. 10. We know that β is smaller, the braking torque is greater, while in actual case there is a limit of β.

G_m is proportional to the square of d_m, while it is nearly proportional to θ, then it will be recommended to finely adjust the load character by means of the adjustment of θ.

5. Foundamental Equation of Performance.

When the disc is rotating at a constant speed, we have

$$\Psi_{it}+\Psi_l+\Psi_f+\Psi_m+\Psi_{bp}+\Psi_{bq}=0 \quad \cdots\cdots\cdots (53)$$

where Ψ_l denotes the torque due to the light load compensation, the frictional torque, which can be written

$$\Psi_f = -(\Psi_{fs}+k_f f_{it}) \quad \cdots\cdots\cdots\cdots (54)$$

while the second term is slightly dependent on the load character, then putting

$$C_l = \frac{\Psi_l-\Psi_{fs}}{\Psi_d} \quad \cdots\cdots\cdots\cdots (55)$$

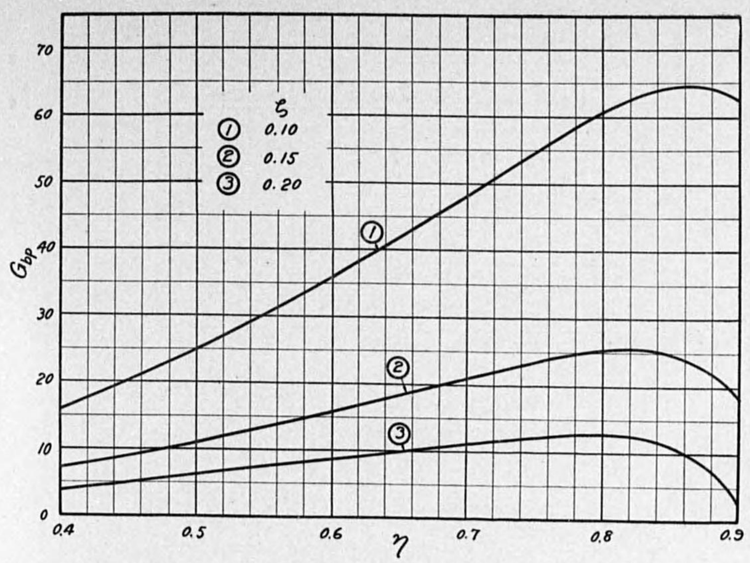

Fig. 9A

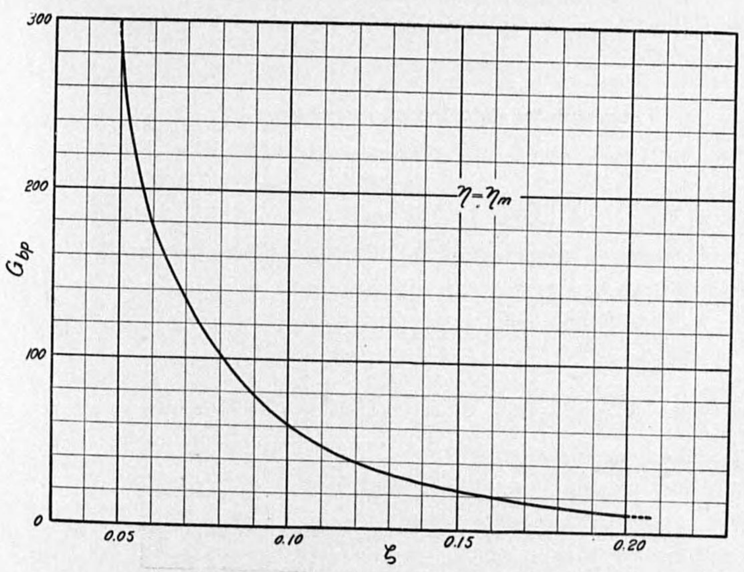

Fig. 9B

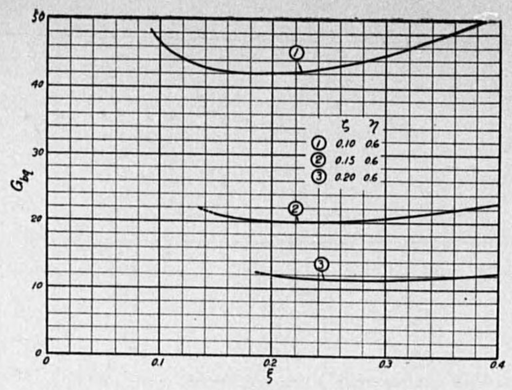

FIG. 9C

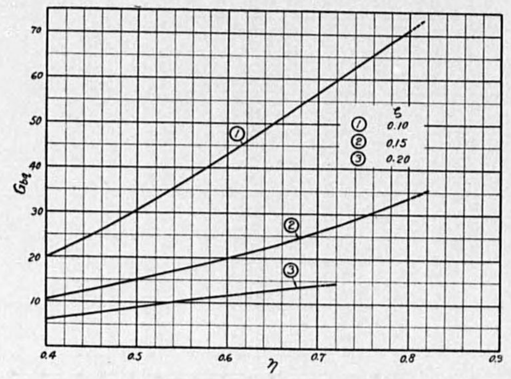

FIG. 9D

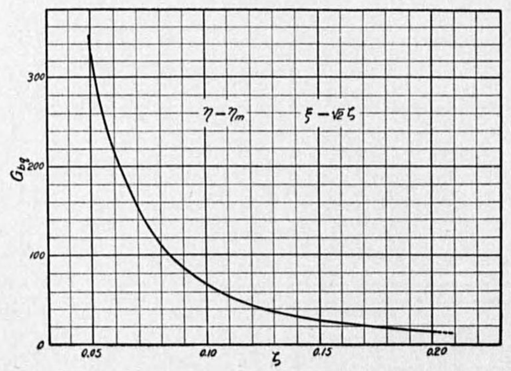

FIG. 9E

TABLE IIA.

$G_{\eta p}$.

η \ ζ	0.05	0.10	0.15	0.20
0.4	64.0	16.0	7.07	3.96
0.5	99.9	24.9	11.0	6.14
0.6	144.	35.7	15.7	8.68
0.7	195.	48.1	20.9	11.3
0.8	253.	60.9	25.3	12.8
0.9	306.	62.9	17.8	2.07

TABLE IIB.

$G_{\eta q}$.

	ζ=0.05					
η \ ξ	0.05	0.0707	0.10	0.20	0.30	0.40
0.4	81.4	74.4	72.4	81.3	101	123
0.5	126.	115.	110.	118.	137	164
0.6	182.	165.	158.	162.	181	208
0.7	247.	223.	213.	214.	232	257
0.8	322.	290.	275.	271.	286	304
0.9	398.	350.	326.	309.	280	—
	ζ=0.10					
η \ ξ	0.10	0.1414	0.20	0.30	0.40	—
0.4	21.4	20.3	21.3	25.5	32.1	—
0.5	32.7	30.5	30.8	34.6	41.0	—
0.6	46.5	42.9	42.2	44.4	51.2	—
0.7	62.8	57.0	55.0	57.2	62.0	—
0.8	79.6	70.9	67.0	66.5	64.1	—
0.9	—	—	—	—	—	—
	ζ=0.15					
η \ ξ	0.15	0.20	0.2121	0.30	0.40	—
0.4	10.2	10.2	10.3	11.6	14.3	—
0.5	15.2	14.6	14.7	15.7	18.2	—
0.6	21.3	20.0	19.9	20.4	22.4	—
0.7	28.0	25.5	25.4	27.9	25.9	—
0.8	33.2	29.2	28.7	—	—	—
0.9	—	—	—	—	—	—
	ζ=0.20					
η \ ξ	0.20	0.2828	0.30	0.40	—	—
0.4	6.26	6.61	6.77	8.11	—	—
0.5	9.02	8.98	9.09	10.2	—	—
0.6	12.3	11.7	11.6	12.2	—	—
0.7	15.2	13.9	13.7	—	—	—
0.8	—	—	—	—	—	—
0.9	—	—	—	—	—	—

TABLE IIIA.

K_p.

η \ ζ	0.05	0.10	0.15	0.20
0.4	3.31	1.69	1.17	0.934
0.5	4.13	2.12	1.49	1.20
0.6	4.99	2.58	1.83	1.51
0.7	5.83	3.08	2.25	1.91
0.8	6.76	3.72	2.90	—
0.9	8.14	—	—	—

TABLE IIIB.

K_q.

η_1 \ ζ	0.05	0.10	0.15	0.20
0.4	7.69	4.30	3.41	3.12
0.5	9.52	5.20	3.97	3.51
0.6	11.4	6.20	4.65	4.06
0.7	13.3	7.29	5.47	4.70
0.8	15.5	8.67	6.58	—
0.9	18.6	—	—	—

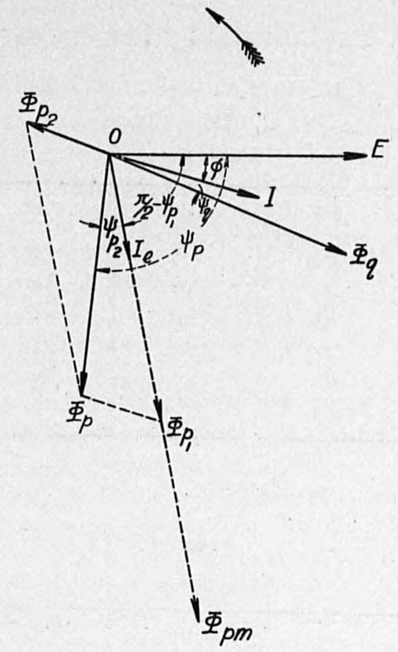

FIG. 11.

As shown in Fig. 11, we have

$$\left.\begin{aligned}\boldsymbol{\Phi}_p &= K_p E e^{j\omega t}\\ \boldsymbol{\Phi}_q &= K_q I e^{j(\omega t-\phi)}\end{aligned}\right\} \quad \cdots\cdots\cdots\cdots\cdots\cdots \quad (56)$$

Therefore the foundamental equation of performance can be written

$$f_d = f\frac{G_d}{G_m}\frac{K_p K_q}{\boldsymbol{\Phi}_m^{\,2}} EI\sin(\psi_p-\psi_q-\phi)\cdot(1+C_f-C_p-C_q) \quad . \quad (57)$$

where C_f, C_p and C_q are dependent on E or I and K_p, K_q, ψ_p, ψ_q are also dependent on E and I as resolved in the latter chapters.

CHAPTER IV. EXPERIMENTAL STUDY ON DRIVING TORQUE.

1. Experimental Study on Flux Distribution.

As mentioned already, the geometricaal constant proposed by the author is an important factor. This constant will enable us to justify how efficiently the magnetic flux are used. This constant is closely related to the dimension of flux-boundary as well as the configuration of flux-distribution. In the above chapter, the author has been shown this constant where the flux are uniformly distributed in the circles. However, in actual case the above assumption shall not be held, therefore the mathematical solution can not be practicable, while the results will be still available as a compass for the design as well as the improvement of the meter.

The geometrical costant is closely connected with the configuration of flux-distribution, then in this chapter firstly this point will be investigated about various meters.

In the experiment, the modified a. c. potentiometer as shown in Fig. 12 is used, where N_s is a search coil, G vibration galvanometer, M variable mutual inductance, and r_1, r_2 non-inductive variable resistances.

Let B_p, B_q be the density of pressure flux or that of current flux, and ψ_p, ψ_q the phase angle between E and B_p or I and B_q respectively, then from the condition of balance, it follows

$$\left.\begin{aligned} B_p &= \frac{\sqrt{\rho^2+\omega^2M^2}}{4.44fA_sN_s}\cdot\frac{E}{R}\cdot 10^8 \\ \psi_p - \pi/2 &= \tan^{-1}\omega L/\rho \end{aligned}\right\} \quad \cdots\cdots\cdots (58)$$

$$\left.\begin{aligned} B_q &= \frac{\sqrt{\rho^2+\omega^2M^2}}{4.44fA_sN_s}\cdot I\cdot 10^8 \\ \psi_q &= \tan^{-1}\rho/\omega L \end{aligned}\right\} \quad \cdots\cdots\cdots (58)$$

where

$$\rho = r_1 r/(r+r_1+r_2), \quad \text{or} \quad r_1 R/(R+r_1+r_2)$$

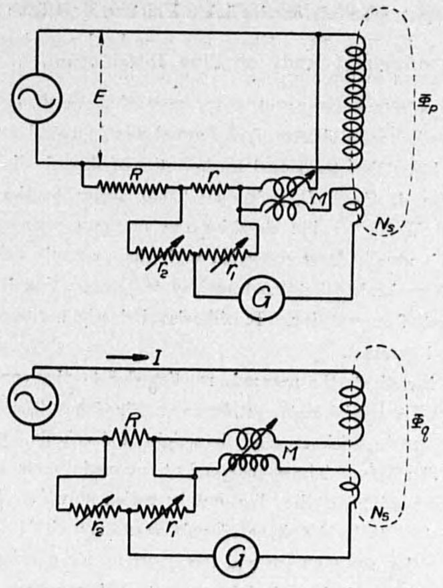

Fig. 12.

The search coil is wound in a form of ellipse, 3 mm in length and 2 mm in width and has 20 turns of enameled copper wire S. W. G. 48. The effective area of coil A_s is determined by the comparison with a standard search coil, because the determination of the area from the dimension will not be satisfactory. The standard coil has 5 turns of S. W. G. 45 silk-covered copper wire wound on a circular thin ebonite disc, 0.936 cm in diameter 0.6788 cm² in effective area. These two coils are placed in the uniform magnetic field due to a solenoid and a variable mutual inductance is connected in series to the solenoid. The induced electromotive force in each coil is measured by the mutual inductance and a vibration galvanometer. These electromotive forces are, of course, proportional to the product of the effective area and the number of turns of coil, hence the effective area of the coil under test can be easily obtained. In our experiment, A_s is 0.04905 cm².

The measurements are made on the finished meters, type from A to G. These results are shown in Fig. 13. There are some local secondary reactions due to the metallic substances in the air gap. In order to eliminate these reactions from the results, the quadrature component of pressure flux to E, B_{pj} and the same phase component of current flux to I, B_{qi} are shown in the above results. From these results, we know that the actual configuration of flux-distribution is complicate. Especially at Type A, C and D, it is remarkable, owing to the influence of the magnetic shunt. While the flux densities are nearly constant within a certain boundary which is usually large compared with the magnetic pole. At Type D and E, it will be noticeable that the boundary of pressure flux is remarkably large compared with that of current flux. It will arise obviously a remarkable consequence on the geometrical constant.

In order to investigate the magnetic reaction due to the current in the disc, the author designed a special meter as shown in Fig. 15. The disc is 4.5 cm in radius and 0.118 cm in thickness, and the weight of disc is 25.6 gr and the moment of inertia is 157.8 cm^{2}gr. Three independent magnetic poles are arranged and these positions respecting to the disc can be varied at will. The cores of poles are made of soft iron to be the shape of pole as nearly circle as passible. The radius of these poles are 0.45 cm and the length of air gap is 0.2 cm. In the experiment, the middle pole is excited by an alternating current, 0.6 ampere and 50 cycle, and the outside poles are removed. The experimental results are shown in Fig. 14. The flux-distribution along X-axis is symmetrical, while that along Y-axis is slightly unsymmetrical, owing to the stray magnetic flux from the core. It can be considered that the flux densities are nearly constant in a circular boundary, and it is obvious that the magnetic reaction due to the eddy current B_2 is not remarkable. However, the phase angles between the applied flux and the resultant flux ψ_2 is not constant everywhere, although they are constant under the pole. But it will not give any remarkable influence upon the torque, because the flux densities are very small outside of the considered boundary. However, the slight deviation between the configuration of flux-distribution supposed and that in actual state will give a remarkable difference between these torques at the extreme case where the poles are placed very near the edge of disc. So that it will not be agreeable to compare them at such a case.

2. Method for Measurement of Driving Torque.

The most usual instrument of measuring torque is a torsion balance which depends on the torsion of fine spring. This instrument will not be reliable owing to the elastic fatigue of spring. The author designed a torque meter as shown in Fig. 16, based on the dynamical balance. In this meter, a magnifying lens and a scale with a vernier are provided to obtain the precise reading. The weights from 0.1 to 10 gr are prepared and the angle can be measured with the accuracy of 10 minutes. If the balance take place at 45°, the accuracy in torque is about 0.3 %.

3. Experimental Results.

In order to verify the theoretical results in the chapter II, the experiment is made on the special meter as shown in Fig. 15. The driving torque can be calculated by the equations (15), (16) and (17), supposing that $\sigma=3.4\cdot10^{-4}$ and $\zeta=(a_c+\delta_g)/R \fallingdotseq 0.15$ where a_c denotes the radius of pole and δ_g the length of air gap.

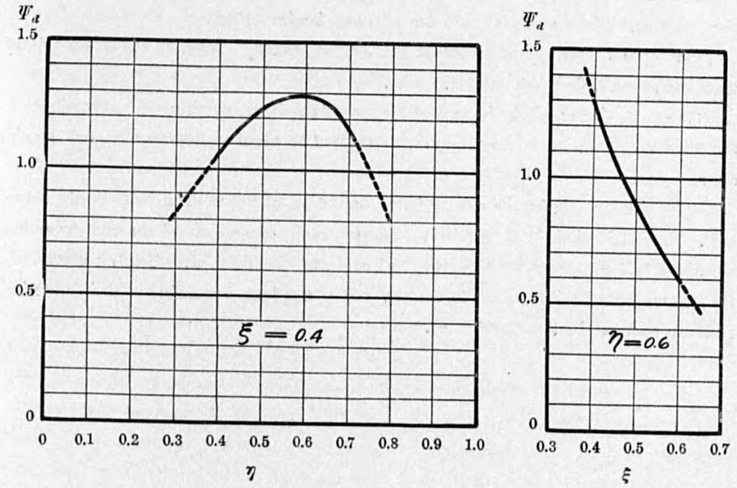

Fig. 17.

The calculated values and the measured values of torque are assembled in Table IV. We know that these values are in sufficiently close agreement with each other, excepting the extreme case.

The same measurements are made on the finished meters, and the geometrical constants are calculated by the following equation,

$$G_d = \frac{g\Psi_d}{2\sigma c f \Phi_p \Phi_q}$$

These results are assembled in Table V. According to these constants and the configuration of flux-distribution, we can criticize on the driving torque.

In Type *D* and *E*, the geometrical constants are very small. It is, of course, resulted from that the boundary of flux-distribution is remarkably large. In order to utilize the large pressure flux unless the retarding torque due to this flux increases, it may be considered to enlarge the boundary area of pressure flux. But the author does not recommend such a scheme, because the driving torque does not increase proportionally, owing to that the geometrical constant G_d decreases, and on the other hand, the voltage character will not be important.

In Type *C*, the geometrical constant is remarkably large. It is caused by that the current flux cut twice the disc.

We will know that the geometrical constant is nearly inverse proportional to the relative dimension of boundary with respect to the disc, excepting some special cases.

The similar relation as shown in the equation (20), will be held in the actual case. As it is obvious in Table V, the geometrical constants in actual case are usually small compared with the theoretical values in Table I. The author thinks that it will not be impossible to improve these constants according to the theoretical results presented in the chapter II.

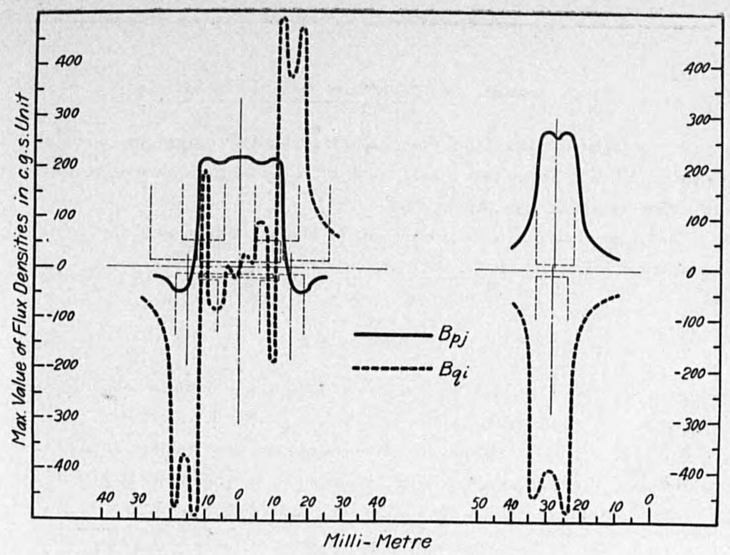

Fig. 13A

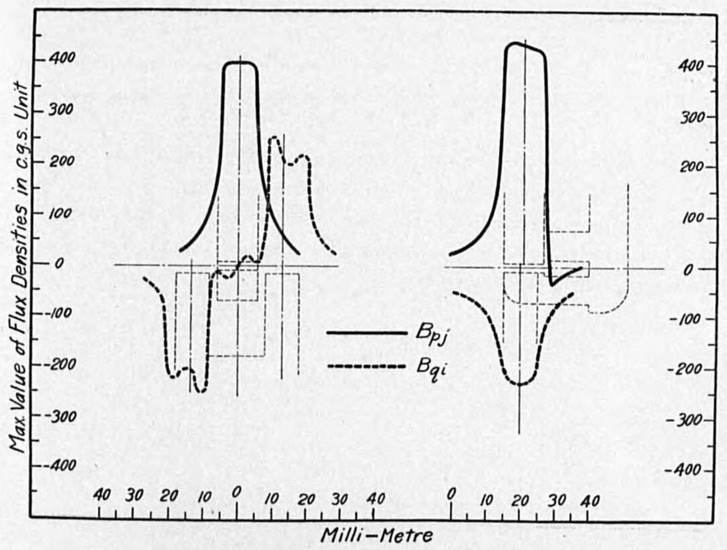

Fig. 13B

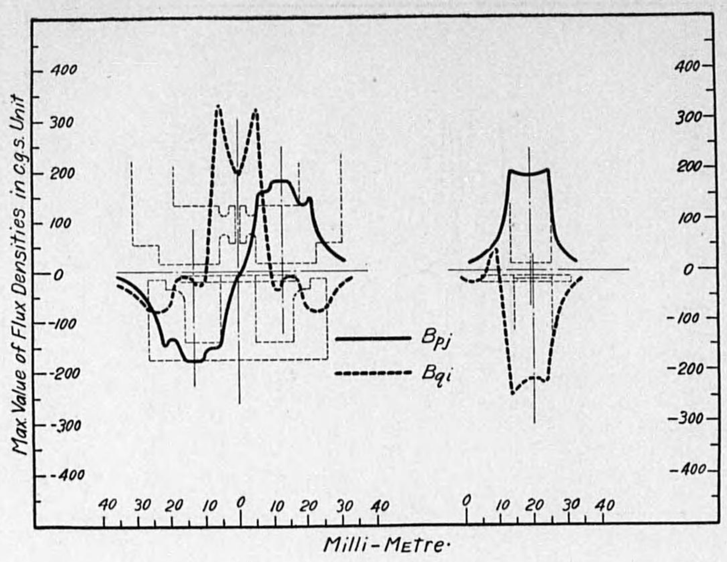

FIG. 13C

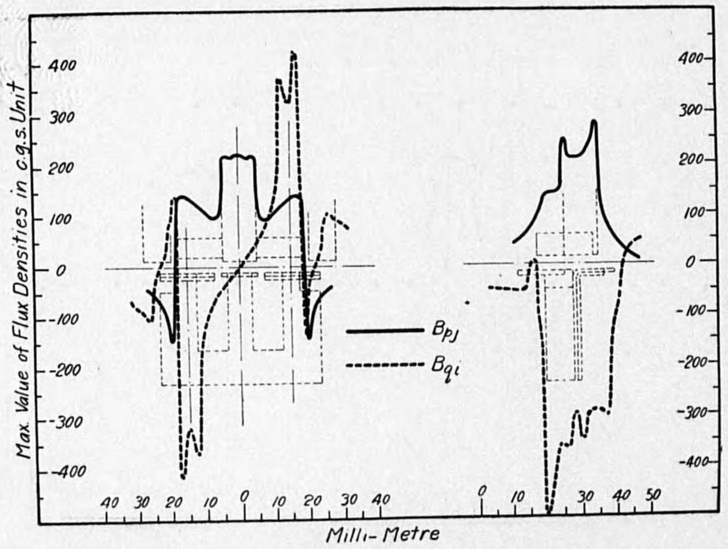

FIG. 13D

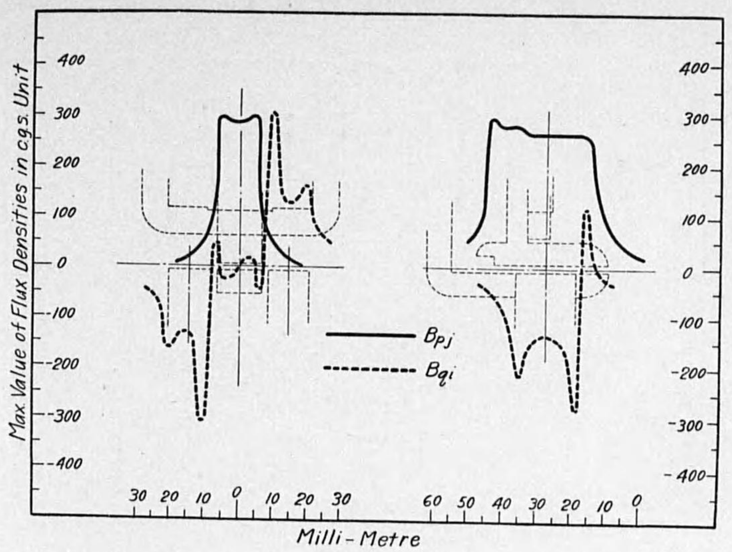

FIG. 13E

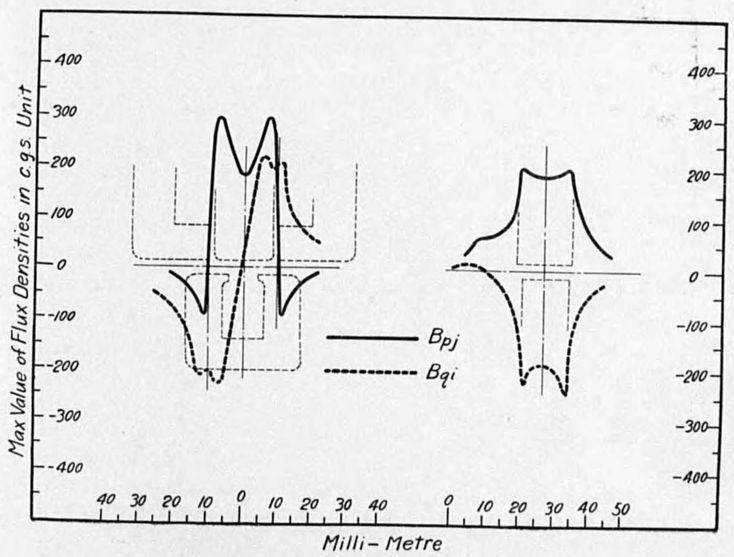

FIG. 13F

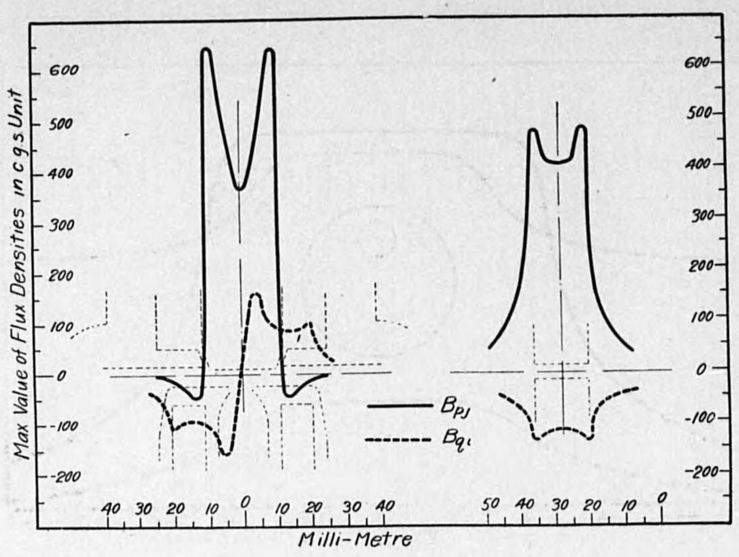

FIG. 13G

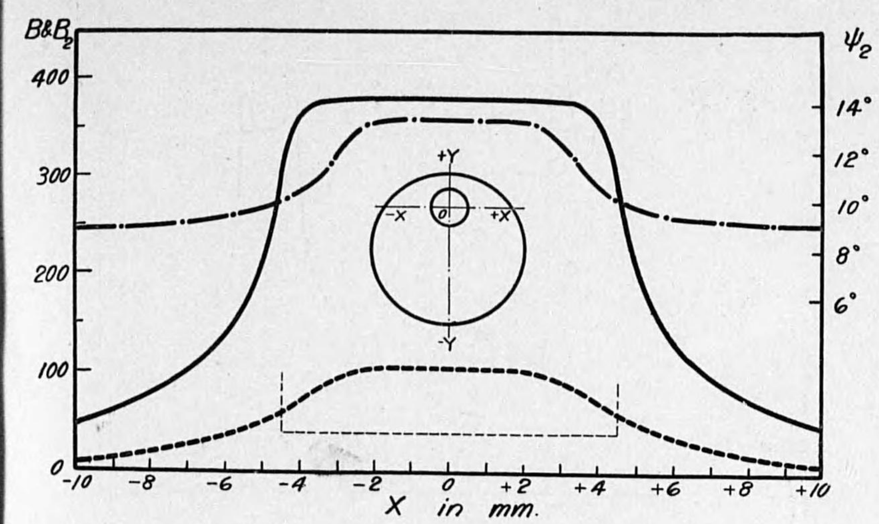

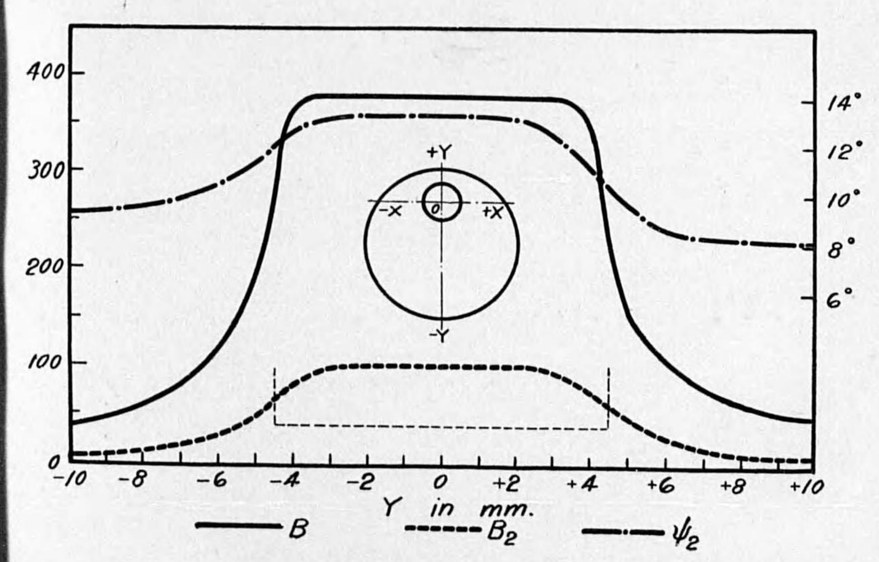

FIG. 14,

Fig. 15

Fig. 16B

Fig. 16A

Fig. 18b

TABLE IV.

$\xi=0.4$

η	0.4	0.5	0.6	0.7
Φ_p	$500._5$	$503._7$	$510._9$	$516._2$
Φ_q	$475._8$	$488._3$	$487._2$	$492._9$
Ψ_d (measured)	1.06	1.23	1.29	1.16
Ψ_d (calculated)	0.76_1	0.91_8	1.00_5	0.96_1
Ratio	1.39_2	1.34_0	1.28_4	1.20_7

TABLE V.

Meter	c	f	Φ_p	Φ_q	Ψ_d	G_d
	cm	~			cm-gr	
A	0.12	50	1,570	830	4.78	0.88
B	0.13	60	1,290	620	4.15	0.96
C	0.13	60	730	670	2.85	1.03
D	0.14	50	1,550	900	4.74	0.70
E	0.12	50	2,280	760	4.66	0.63
F	0.08	60	1,180	1,030	3.61	0.89
G	0.06,	60	3,410	820	5.38	0.70

CHAPTER V. EXPERIMENTAL STUDY ON RETARDING TORQUE.

1. Method for Measurement of Retarding Torque.

In this chapter, the frictional torque and the retarding torque due to the alternating magnetic flux will be investigated experimentally.

There are the few literatures[3][10] on the method of measuring the frictional torque, while any methods have not been available for the measurement of the electromagnetic retarding torque.

The author proposes a method in which the retardation of revolving disc can be automatically recorded. This method bases on the utilization of photo electric cell as shown in Fig. 18. In this method, a bridge consists of a photo electric cell, a variable high resistance R_2 and two batteries E_1 and E_2. When the photo cell is not exposed, E_2 is so adjusted to impress a sufficient negative potential on the grid of triode valve to be the plate current nearly zero. When the beam of light reflected from the mirror on the spindle of disc falls on the photo cell, the internal resistance of cell will quickly decrease; in this case, if the internal resistance of cell is nearly equal to R_2E_1/E_2, the grid potential becomes zero, and the current

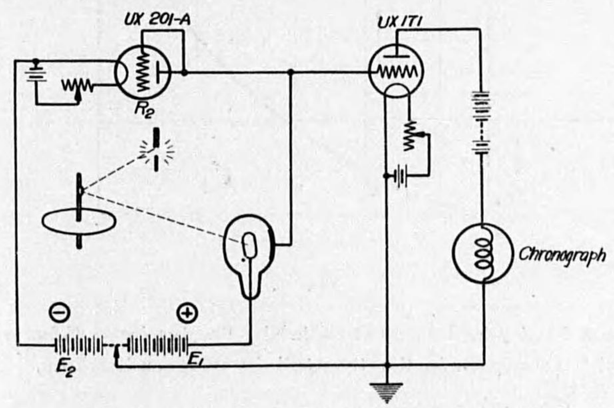

FIG. 18A

sufficient to record a dot on the paper flows through the striker of chronogragh in the plate circuit.

Fig. 19 shows the relation between the number of revolutions of disc N_1 and the time t_1. The method of computing the frictional torque from this relation has been already known; however, the method available for the retarding torque has not been found. Now the author proposes the following method of computation of retarding torque.

In Fig. 19, O_1 denotes the beginning of record and O_2 the point at which the disc stopped. It is difficult to determine the point O_2, and only a portion of the retardation curve OO_2 can be obtained.

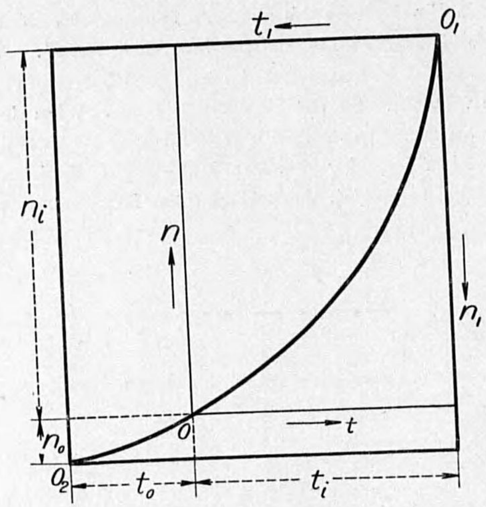

FIG. 19.

Let α, β and γ be the moment of inertia, the damping coefficient and the frictional torque respectively, then the retardation curve can be written,

$$\frac{d^2n_1}{dt_1^2}+\delta\frac{dn_1}{dt_1}+\delta\ v=0$$

where $\delta=\beta/\alpha$ and $v=\gamma/\beta$.

From this equation, we have

$$n_1=A_1e^{-\delta t_1}+B_1-vt_1$$

where A_1 and B_1 are integral constants.

To transfer the origin from O_1 to O, putting

$$t_1=t_i-t$$

$$n_1=n_0+n$$

Then it follows

$$n=Ae^{\delta t}+B+vt$$

From the following conditions,

$$t=0,\quad n=0\quad\text{and}\quad t=t_i,\quad n=n_i$$

we have

$$n=n_a(e^{\delta t}-1)+vt$$

where

$$n_a=(n_i-vt_i)/(e^{\delta t_i}-1)$$

In our case, the second term will be negligible small, so long as t is not too small. Hence, we have

$$\delta t=2.3\log_{10}(1+n/n_a)\qquad\cdots\cdots\cdots\cdots\cdots\quad(59)$$

where n_a is usually from 0.5 to 2.0 in actual case, then by means of trial method using a semi-logarithmic section paper, the value of n_a satisfying the above relation can be easily determined. When the relation is satisfied, the retarding torque can be given by $f_a\alpha\delta$ in cm-gr.

In the measurement of moment of inertia α, a disc is suspended by a fine strip, and two metallic rings are prepared. By the substitution method, the

moment of inertia of disc can be determined from the period of oscillation at each case where one of the rings is mounted on the disc.

For the computation of frictional torque, the author adoptes the method already known.[3]

2. Frictional Torque.

As mentioned already, the frictional torque Ψ_f is given by

$$\Psi_f = -(\Psi_{fs} + k_f f_d) \quad \cdots\cdots\cdots\cdots\cdots\cdots \quad (54)$$

The starting torque Ψ_{fs} is chiefly caused by the friction between jewel and pivot or ball, and k_f is arisen from the air friction on the rotating disc, which is nearly proportional to the surface of disc, by the previous paper.[4]

There is no need to attend to the latter, because it scarcely affects on the load character, while the former gives a remarkable effect on the load character at light load. In some paper,[10][24] it has been obtained that the starting friction is proportional to W where W den tes the weight supported by the pivot.

A series of measurement are made of the relation between the starting torque and the weight of moving part about various kinds of bearing. In our experiment, the rotating disc is 8.5 cm in diameter and 0.14 cm in thickness, and many sheets of tin-foil which have the same dimension as that of the disc, are provided to obtain the different loads.

The results are shown in Fig. 20, and the empirical formula for each kind of bearing are given as follows,

$$\left.\begin{aligned} \Psi_{fs} &= 0.0264\ W^{1.44} \cdot 10^{-3} \text{ in cm-gr} \quad \text{for pivot bearing} \\ \Psi_{fs} &= 0.0421\ W^{1.45} \cdot 10^{-3} \text{ in cm-gr} \quad \text{for semi ball pivot bearing} \\ \Psi_{fs} &= 0.1343\ W \cdot 10^{-3} \text{ in cm-gr} \quad \text{for ball bearing} \end{aligned}\right\} \quad (60)$$

The above results for the pivot bearing are in sufficiently close agreement with the previous results.

It will be noticeable that the performance of semi ball pivot bearing is similar to that of pivot bearing, while the frictional torque in the former is slightly large compared with that in the latter, because the surface of ball touching jewel is

usually greater than that of pivot. While there are troublesome in finishing the pivot, therefore the semi ball pivot bearing will be recommended in our case.

The ball bearing is suitable for the large load, while in our case the weight of moving part is not large, then the ball bearing will not be recommended in our case.

3. Retarding Torque.

In order to verify the theoretical results in the chapter III, the measurement of retarding torque is made of the special meter as shown in Fig. 15. Firstly, the middle pole is excited by the alternating current which is so adjusted that the total flux at the pole are always 500. Secondly, the outside poles are similarly excited. The experimental results are shown in Fig. 21.

On the other hand, the torques are calculated by the equations (32), (33),

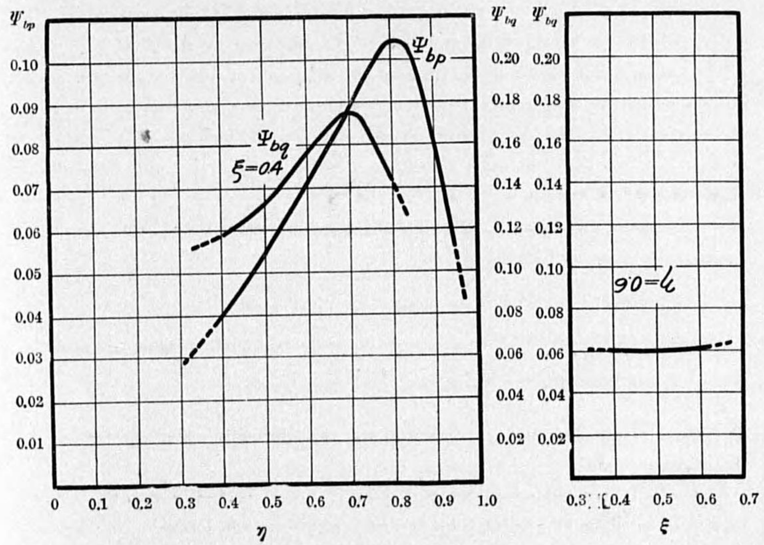

Fig. 21.

(34) and (35) respectively. These results are assembled in Table VI. At Type *F* and *C*, the pressure flux cut twice the disc as shown in Fig. 13. Then in these types the geometrical constants G_{bp} are large. At Type *B*, this constant is large, owing to the small boundary of flux-distribution. At Type *D*, *E*, these constants are remarkably small, owing to the large boundary of flux-distribution. It is noticeable that at Type *G* the constant is very small in spite of twice cutting of flux through the disc. It will be arisen from that the flux density is remarkably small under the centre of pole where the current density will be maximum. Such a configuration of flux-distribution on the stand-point of the retarding torque as well as the driving torque will be recommended.

The geometrical constant G_{bq} is greatest at Type *G*, and at Type *A* and *D* these come next. It will result from steeply changing in the direction of flux. However, there is not a remarkable variation in the series of these constants.

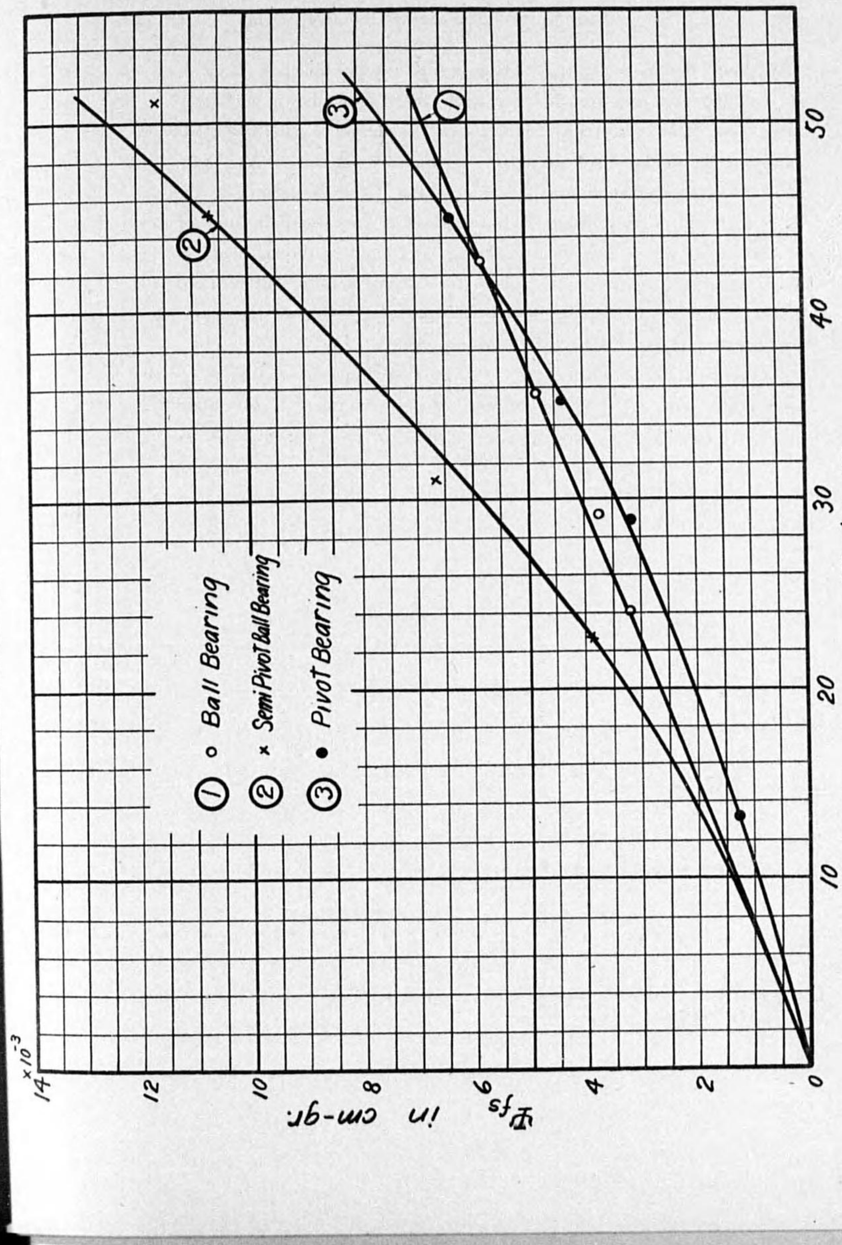

Fig. 20.

TABLE VI.

$f_d = 1$ r.p.s.

Ψ_{tp} \ η	0.4	0.5	0.6	0.7	0.8
Measured Value	0.040 cm-gr	0.05_3	0.07_0	0.08_8	0.10_4
Calculated Value	0.037 cm-gr	0.05_7	0.08_1	0.10_7	0.13_0
Ratio	1.0_8	0.9_3	0.8_6	0.8_2	0.8_0

$\xi = 0.4$ $\quad f_d = 1$ r.p.s.

Ψ_{tq} \ η	0.4	0.5	0.6	0.7
Measured Value	0.12 cm-gr	0.13_2	0.15_8	0.17_3
Calculated Value	0.15 cm-gr	0.18_6	0.22_9	0.26_4
Ratio	0.8_0	0.7_1	0.6_9	0.6_6

TABLE VII.

Meter	f_d	Φ_p	Ψ_{bp}	G_{bp}
	r. p. s.		cm-gr	
A	1.11	1,570	0.226	4.0
B	1.00	1,290	0.238	6.3
C	0.69	730	0.093	5.6
D	0.89	1,550	0.169	3.3
E	0.60	2,280	0.189	2.9
F	0.56	1,180	0.087	8.0
G	0.25_5	3,410	0.119	3.5

Meter	f_d	Φ_q	Ψ_{bq}	G_{bq}
	r. p. s.		cm-gr	
A	1.11	830	0.259	8.1
B	1.00	620	0.119	6.9
C	0.69	670	0.055	7.9
D	0.89	900	0.328	9.4
E	0.60	760	0.122	7.8
F	0.56	1,030	0.079	4.8
G	0.25_5	820	0.042	10.5

Meter	K_p	K_q
A	1.14	4.6
B	1.64	3.6
C	1.36	3.8
D	1.18	6.6
E	1.14	6.5
F	2.23	2.7
G	1.24	7.8

CHAPTER VI. STUDY ON LOAD CHARACTER.

1. Equation of Load Character.

Among various characters of watthour meter, the load character will be most important, while the equations of this character presented hitherto are too simple to explain the actual character. The author now presents a complete equation.

The fundamental equation of performance has been already obtained, that is

$$f_d=\sigma c f\frac{G_d}{G_m}\cdot\frac{K_p K_q}{\Phi_m^2}\cdot EI\sin(\psi_p-\psi_q-\phi)\cdot(1+C_f-C_p-C_q) \quad (57)$$

In this time, E and f are constant, and ϕ is zero.

Putting

$$C_f=a/p, \quad \text{and} \quad C_q=a_3p^2 \quad \ldots\ldots\ldots\ldots (61)$$

where p is the ratio of any load current to the rated current. K_q is not constant and it will depend on the magnetic permeability at the path of current flux; in other words, the magnetic saturation. Hence, K_q can be expressed by

$$K_q=k(1+a_1p-a_2p) \quad \ldots\ldots\ldots\ldots\ldots (62)$$

Supposing that K_p, ψ_p and ψ_q are constant, then the equation (57) becomes

$$f_d=K_p(1+a_1p-(a_2+a_3)p+a_f/p)$$

Therefore the load character is given by

$$\varepsilon=\varepsilon_0+a_1p-(a_2+a_3)p+a_f/p \quad \ldots\ldots\ldots\ldots (63)$$

This equation will be available in practice.

2. Experimental Analysis of Load Character.

In order to ascertain the above equation, the relation between the driving torque and the load current is measured. These results are shown in Fig. 23. From these results, we know that the driving torque does not follow the load current, and the

relation is similar to the saturation curve. Supposing that the relation between the driving torque and the load current result from that between K_q and the load current, we can determine the coefficients a_1 and a_2. The coefficient a_3 can be obtained from the experimental results already mentioned. Applying these coefficients into the equation (63), the error can be estimate, considering that a_1/p is negligible small at the heavy load.

The errors estimated and measured are assembled in Table VIII. These values are in sufficiently close agreement with each other.

Strictly speaking, the above relation between the driving torque and the load current will result from the following factors,

(a) the relation between Φ_p, ψ_p and p,
(b) the relation between Φ_q, ψ_q and p,
(c) the relation between the geometrical constant G_d and p.

Now, the experimental analysis are performed as follows,

(a) It will be quite difficult to analyse the relation between Φ_p, ψ_p and p, because the pressure flux and the current flux coexist in the air gap. H. Schering

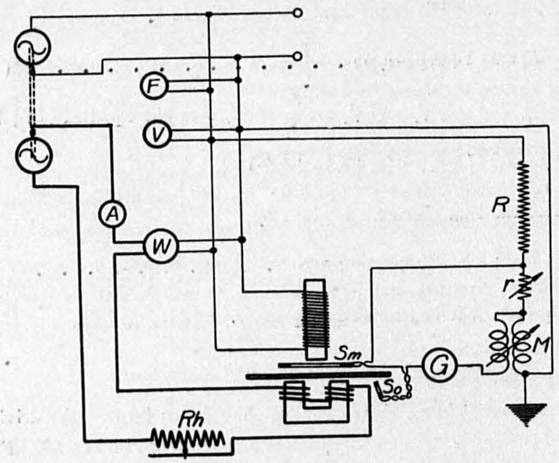

Fig. 25A.

and R. Schmidt have shown a work[7] on this point, while the method will be troublesome. The author succeeds in this analysis by using a simple method as shown in Fig. 25 A.

In this figure, R is the non-inductive resistance, r the variable resistance, M the variable mutual inductance, G the vibration galvanometer. A main search coil S_m is to be placed at the middle point of the pole arrangement. If the current flux are distributed symmetrically, the electromotive force due to the current flux shall be zero. While actually this coil is not free from the electromotive force due to the slight unsymmetry in the current flux. To compensating this electromotive force, an auxiliary search coil S_0 is used, and the compensation can be readily obtained by placing S_0 at such a position that it will interlink the current flux only. Strictly speaking, a perfect compensation can not expected, unless the phase relation is concerned; while this is not noticeable actually. From the condition of balance, we have

$$\left.\begin{aligned} \Phi_p &= \frac{E\sqrt{r^2+\omega^2M^2}}{4.44fN_sR}\cdot 10^8 \\ \psi_p - \frac{\pi}{2} &= \tan^{-1}\frac{\omega M}{r} \end{aligned}\right\} \quad \cdots\cdots\cdots\cdots (64)$$

where the reactance in the primary coil of M is neglected compared with R. The experimental results are shown in Fig. 26.

From these results, we can speak that the pressure flux Φ_p and the phase angle ψ_p are nearly independent of the load current.

(b) The similar method as shown in Fig. 25 B is applied to investigate the relation between the current flux Φ_q, the phase angle ψ_q and the load current.

In the figure, S_m is a main search coil which is made up of two equal coils wound in opposite direction, and S_0 is an auxiliary search coil to compensate the electromotive force due to the slight unsymmetry of the pressure flux. From the condition of balance, we have

$$\left.\begin{aligned} \Phi_q &= \frac{\sqrt{r^2+\omega^2M^2}}{4.44fN_s}\cdot\frac{\rho}{R}\ I\cdot 10^8 \\ \psi_q &= \tan^{-1}\frac{r}{\omega M} \end{aligned}\right\} \quad \cdots\cdots\cdots\cdots (65)$$

where ρ is the resistance of shunt.

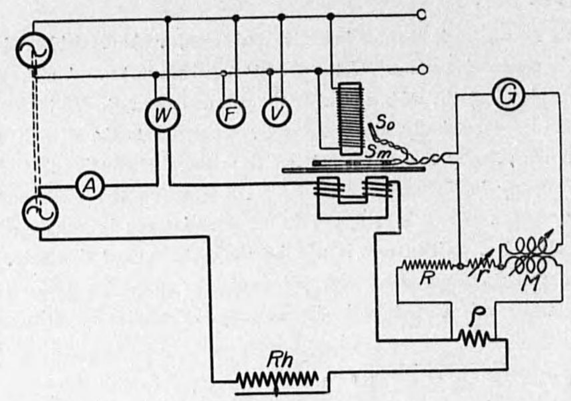

Fig. 25b.

The experimental results are shown in Fig. 27. From these results, we know that the relation between K_q and p are generally similar to that between Ψ_d/p and p.

At Type A and D, this relation is remarkable owing to so called magnetic shunt which is clearly illustrated in Fig. 24. However the magnetic path between two adjacent current poles will generally serve as a magnetic shunt, so that all meters have the similar relation more or less, and this peculiar relation is remarkable in the meter having so-called magnetic shunt.

Now we will consider the relation between ψ_q and p. At Type A and D, a peculiar relation will be found, which is caused by the magnetic shunt. At Type B, a remarkable relation can be found and it will be arisen from the phase compensating coil. Excepting these cases, it can be considered that ψ_q is nearly independent from p.

(c) Now, the relation between the geometrical constant G_d and the load current is investigated. In this time, the configurations of flux-distribution at different currents are required. The method in Fig. 12 will be to complicate in this case.

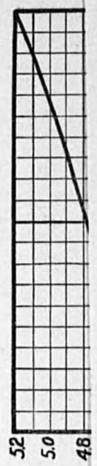

these results, we know
at between Ψ_d/p and p.
to so called magnetic
magnetic path between
ic shunt, so that all
relation is remarkable

At Type A and D, a
ic shunt. At Type B,
he phase compensating
ly independent from p.
and the load current
tribution at different
omplicate in this case.

Fig. 23.

Fig. 22.

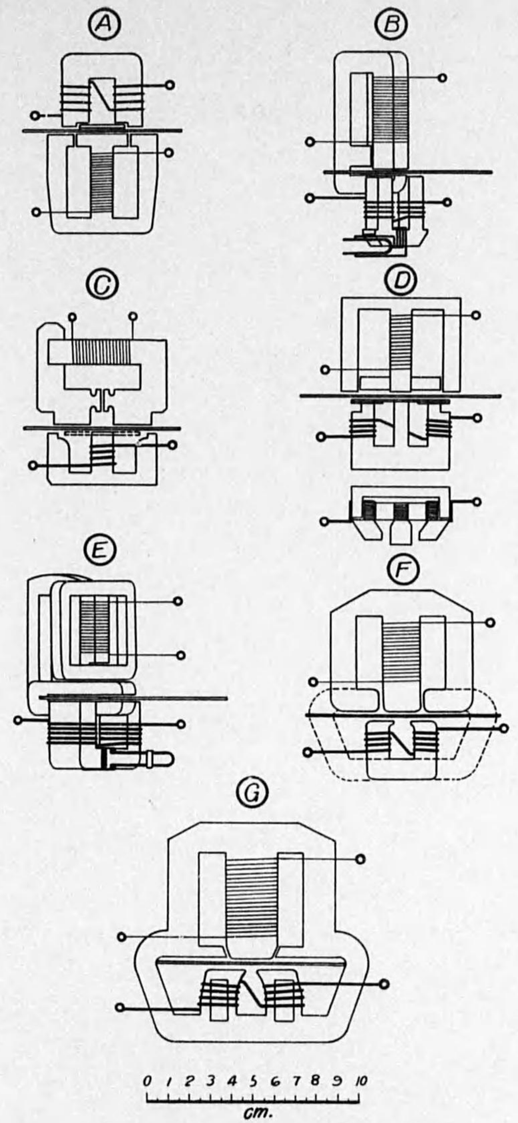

FIG. 24.

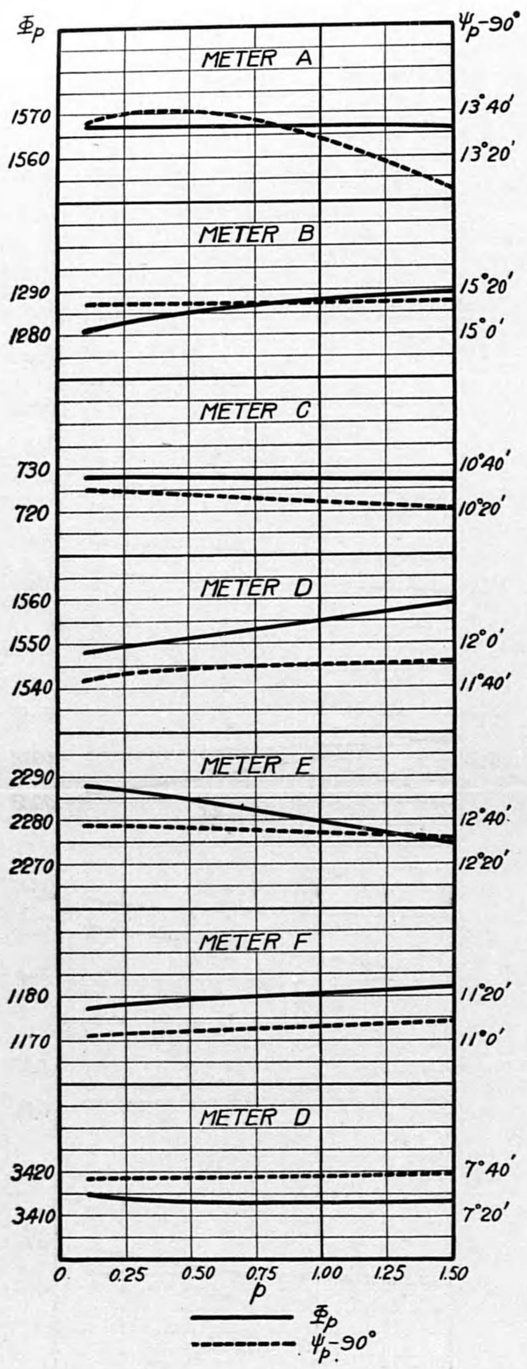
Φp
ψp-90°
METER A
1570
1560
13°40'
13°20'
METER B
1290
1280
15°20'
15°0'
METER C
730
720
10°40'
10°20'
METER D
1560
1550
1540
12°0'
11°40'
METER E
2290
2280
2270
12°40'
12°20'
METER F
1180
1170
11°20'
11°0'
METER D
3420
3410
7°40'
7°20'
0
0.25
0.50
0.75
1.00
1.25
1.50
p
Φp
ψp-90°

FIG. 26.

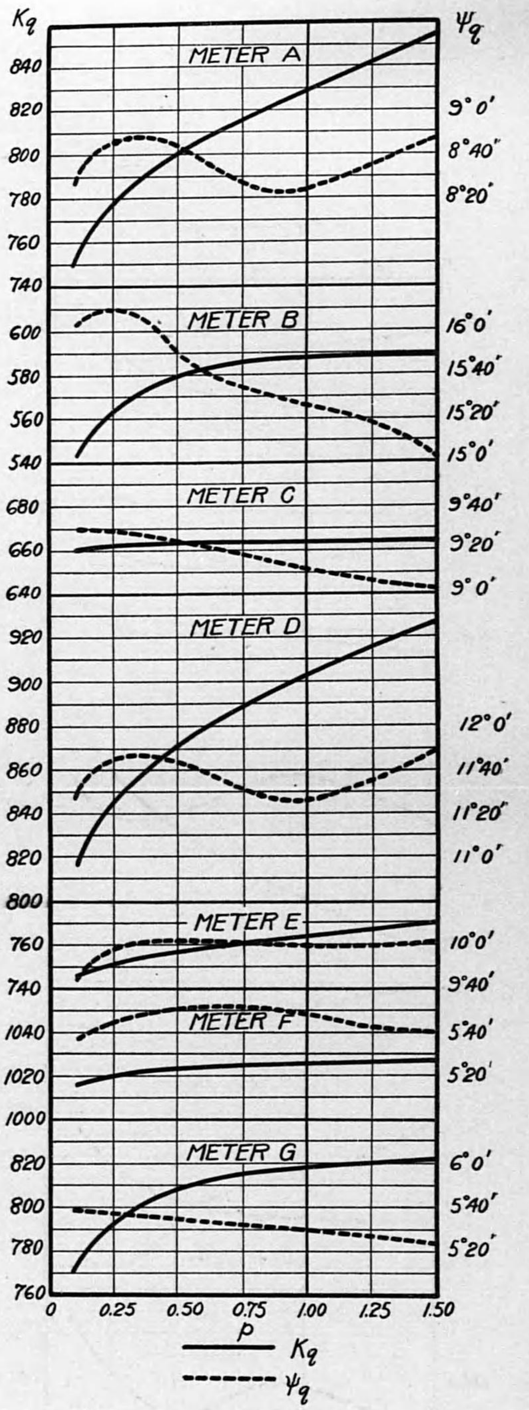
Kq
ψq
METER A
840
820
800
780
760
740
9°0'
8°40'
8°20'
METER B
600
580
560
540
16°0'
15°40'
15°20'
15°0'
METER C
680
660
640
9°40'
9°20'
9°0'
METER D
920
900
880
860
840
820
12°0'
11°40'
11°20'
11°0'
METER E
800
760
740
10°0'
9°40'
METER F
1040
1020
1000
5°40'
5°20'
METER G
820
800
780
760
6°0'
5°40'
5°20'
0
0.25
0.50
0.75
1.00
1.25
1.50
p
Kq
ψq

FIG. 27.

TABLE VIII.

Meter	α_1 in %	α_2 in %	α_3 in %	$p=1.5$ Measured Error	$p=1.5$ Calculated Error	$p=2.0$ Measured Error	$p=2.0$ Calculated Error
				%	%	%	%
A	1.9_4	-2.6_4	5.4_2	−2.3	−2.5	−5.3	− 6.4
B	4.6_3	1.9_1	2.8_7	−3.3	−3.7	−7.5	− 9.7
C	$13._9$	3.4_9	1.9_3	−0.9	+0.2	−2.4	− 2.4
D	$16._1$	3.0_2	6.9_2	−1.7	−4.4	−5.9	−13.7
E	3.5_4	0.0_5	2.6_2	−1.2	−0.6	−3.2	− 4.5
F	$13._3$	4.2_0	2.1_9	−2.0	−1.1	−4.9	− 5.4
G	$12._7$	3.5_6	0.7_8	−0.9	+0.9	−1.0	− 0.3

Hence, a simple method satisfactory to give an outline is used. In the method, the pressure coil is excited by the direct current and the current coil by the required alternating current. An extremely small search coil connected to a vibration galvanometer is slowly displaced with a constant speed, on the other hand, the deflection of galvanometer is recorded on a film wound on a rotating drum which rotates slowly with a constant speed. The working resonant sharpness of vibration galvanometer has to be considerably small. The measuring device has not been completed hitherto, while in the preliminary experiment any remarkable changes in this point can not be found.

After all, we can conclude that the relation between the driving torque and the load current depends chiefly on that between K_q and p, and the load character can be generally represented by the equation (63).

3. Method of Improving Load Character.

The over-load character of meter has attracted a great attention everywhere.

In order to improve the over-load character, the following methods must be used. The first method is to utilize a magnetic shunt. The most important factor, which makes the over-load character worse, is, of course, the coefficient a_3. Then to compensate it, the magnetic shunt must be designed so as the coefficient a_1 is sufficiently large, unless a_2 increases. (Public notice of patent, No. 2036, 1928)

The other method is pertaining to the geometrical constant G_d. By varying G_d with the load current, we can improve the load character, while G_d is the function of ξ, η and ζ. It is quite difficult to vary ζ with the load current, so that G_d must be varied by changing ξ or η. R. M. Fichter has already succeeded in varying η at over load. (Patent No. 72464, 1927)

CHAPTER VII. STUDY ON TEMPERATURE CHARACTER.

1. Equation of Temperature Character.

The temperature character will be also important. The temperature error of meter will be caused by the variation in resistance, magnet and permeability due to temperature change. The last point has not been much concerned hitherto. According to T. Spooner's work,[14] the temperature coefficient of permeability of silicon steel will amount to +0.0012, so long as the flux density is not large. The temperature coefficient of resistivity of copper wire is usually about 0.0043.

Now we can represent the relation between the magnetic flux and temperature as follows,

$$\left.\begin{aligned}\Phi_p &= \Phi_{p0}\,(1+\alpha_p T)\\ \Phi_q &= \Phi_{q0}\,(1+\alpha_q T)\end{aligned}\right\} \quad \cdots\cdots\cdots\cdots\cdots\cdots \quad (66)$$

The magnetic circuit of pressure flux is nearly closed, then α_p is usually greater than α_q.

As it is clear in Fig. 11, we have

$$\psi_p - \pi/2 = \psi_{p2} - \psi_{p1}$$

while $\psi_{p1} = R/\omega L$ and $R = R_0(1+\beta_r T)$, $L = L_0(1+\beta_l T)$

Hence

$$\psi_{p1} = \psi_{p10} + (\beta_r - \beta_l)\,T$$

Putting

$$\beta_{p1} = \beta_r - \beta_l$$

Then we have

$$\psi_{p1} = \psi_{p10} + \beta_{p1} T$$

Similarly

$$\psi_{p2} = \psi_{p20} + \beta_{p2} T$$

Therefore we have

$$\psi_p - \pi/2 = \psi_{p0} - \beta_p T \quad \cdots\cdots\cdots\cdots\cdots\cdots \quad (67)$$

where $\psi_{p0} = \psi_{p20} - \psi_{p10}$ and $\beta_p = \beta_{p1} - \beta_{p2}$

Similarly we hawe

$$\psi_q = \psi_{q0} - \beta_q T \quad \cdots\cdots\cdots\cdots\cdots\cdots \quad (68)$$

Let α_m be the temperature coefficient of brake magnet, then α_m is usually from -0.0005 to -0.0002. Then we have

$$\Phi_m = \Phi_{m0}\,(1-\alpha_m T) \quad \cdots\cdots\cdots\cdots\cdots\cdots \quad (69)$$

From these equations, we can represent the temperature character as following equation,

$$\varepsilon = \varepsilon_0 + (\alpha_p + \alpha_q + 2\alpha_m)\,T - (\beta_p - \beta_q)\tan\phi\;T \quad \cdots\cdots\cdots \quad (70)$$

where ε_0 denotes the error independent of temperature and β_p, β_q are given in radian.

2. Experimental Analysis of Temperature Character.

The experimental analysis on the temperature character is performed as follows. In our experiment, a bath with a thermostat — Bulb mercury type thermo-indicator with electric contact — is used, and an electric heater, Bavaria type refrigerator and temperature recorder are provided in this bath. We can keep the temperature in this bath within the average deviation less than 0.5° C from −30° C to +50° C.

The temperature characters are measured on the finished meters and these results are shown in Fig. 29 and 30.

The temperature coefficients of α_p, α_q, β_p and β_q are measured by a search coil and a portable a.c. potentiometer. These results are shown in Fig. 31 and 32.

The temperature coefficient of brake magnet, which is most important, is measured by a differential method as shown in Fig. 33. In this measuring device, two thin mica discs, in which a semi-circular coil is mounted, are firmly attached to a rotating shaft, and these coils are wound in opposite direction. The difference of

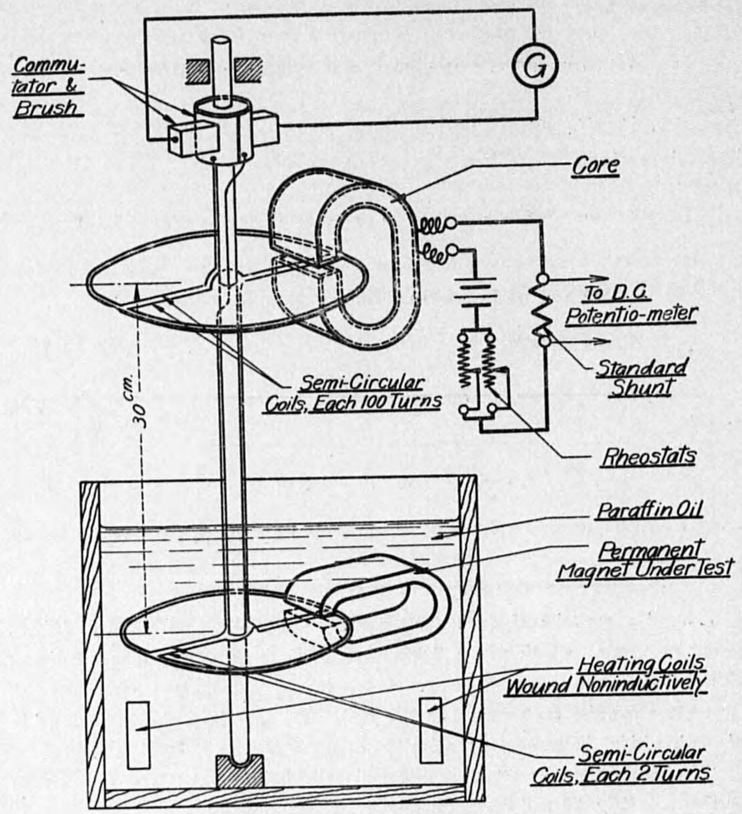

FIG. 33.

electromotive force induced in each coil is rectified by a commutator and then supplied to a long period galvanometer. The magnet under test is placed in a bath filled with paraffin oil whose temperature is controlled by a thermostat. The electric heater in this bath is carefully wound to produce no stray magnetic flux. The upper coil is troidal type, in order to produce no stray magnetic flux.

The change of magnetic flux in the magnet is balanced by adjusting the current through the upper coil which can be precisely measured by potentiometer method. In this method, the precise result can be expected. The experimental results are shown in Fig. 34_A.

From these results, the temperature coefficient at unity power factor $(\alpha_p+\alpha_q+2\alpha_m)$ and that at low power factor, $(\beta_p-\beta_q)\tan\phi$ are separately given. These calculated values are in sufficiently close agreement with those measured.

Therefore the temperature character can be generally represented by the proposed equation (70).

3. Method of Improving Temperature Character.

The temperature coefficients in the standards[18]-[22] of various countries are as follows,

Standard	Temperature coefficient
Japanese	0.1 %
British	0.1 %
U. S. A.	0.12 %
Swiss	0.3 %

In these standards, it is clear how we attach great importance to the temperature character. Now the author is going to explain the method of improviug this character.

The temperature coefficient at unity power factor is $(\alpha_p+\alpha_q+2\alpha_m)$. If we can the temperature coefficient α_m is positive, $(\alpha_p+\alpha_q+2\alpha_m)$ will tend to zero. For this purpose, a magnetic shunt of thermoalloy (Cu 30%, Ni 66.5%, Fe 2.2%) is utilized. This device will be suitable for a double type poles only, hence it will not be recommended for bringing down the production cost. Now the author propose a method which is based on changing the geometrical constant G_m with temperature. This method will be suitable for single pole type.

The author thinks that the temperature coefficient of permanent magnet will result from mechanical cause. In order to ascertain this point, a series of measurements is made on the magnets which are supplied from Nihon Tokushuko Co. The

magnets under test consist of Cl 0.7–0.8%, Si 0.13%, Mn 1.5–2.0%, Cr 3%, and these magnets are quenched at 850° C and annealled at 800° C and matured at 100° C for one hour. The results are shown in Fig. 34_{II}. According to these results, we know that the temperature coefficient is nearly proportional to the ratio of air gap to the total length of magnet. Therefore the air gap of magnet must be as small as possible, in order to improve the temperature coefficient as well as the demagnetizing factor.

The temperature coefficient at low power factor will be improved by diminishing β_p. While $\beta_p=\beta_{p1}-\beta_{p2}$, then we must make β_{p2} to be nearly equal to β_{p1}. This can be realized by means of properly designing the temperature coefficient of time constant at the phase compensating circuit.

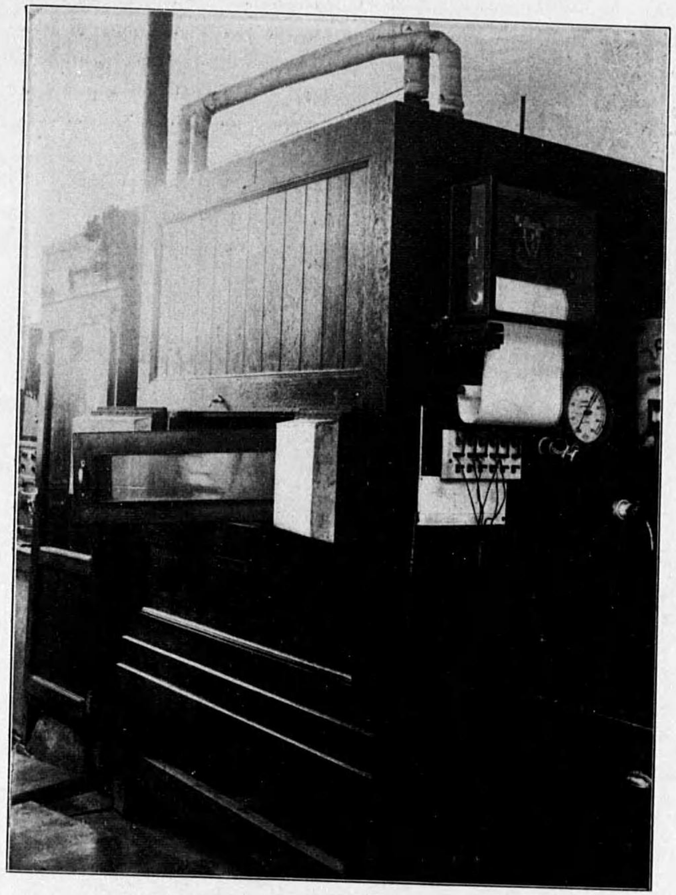

Fig. 28

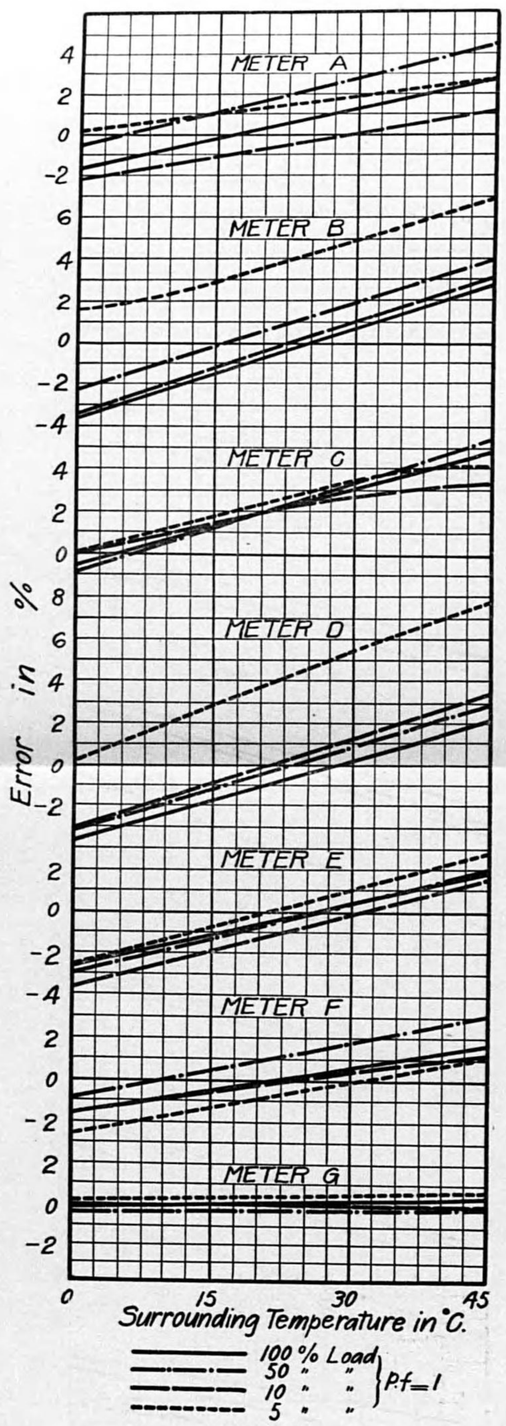
METER A
METER B
METER C
METER D
METER E
METER F
METER G
Error in %
Surrounding Temperature in °C.
0
15
30
45
100 % Load
50 " "
10 " "
5 " "
P.f = 1

FIG. 29.

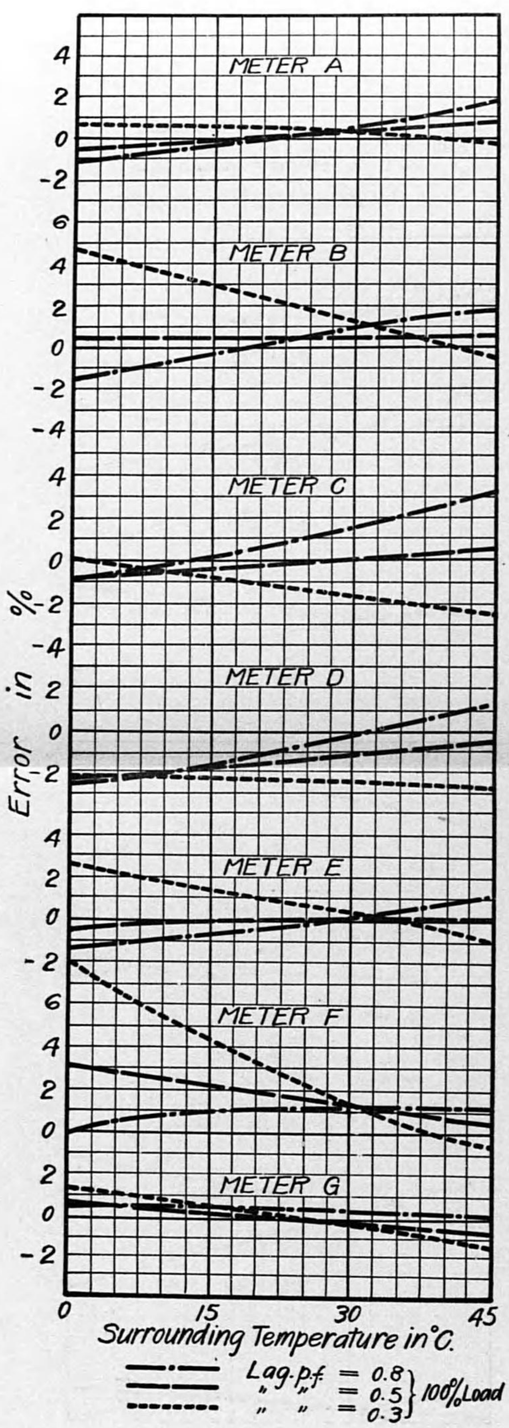
METER A
METER B
METER C
METER D
METER E
METER F
METER G
Error in %
Surrounding Temperature in °C.
0
15
30
45
Lag. p.f = 0.8
" " = 0.5
" " = 0.3
100% Load

FIG. 30.

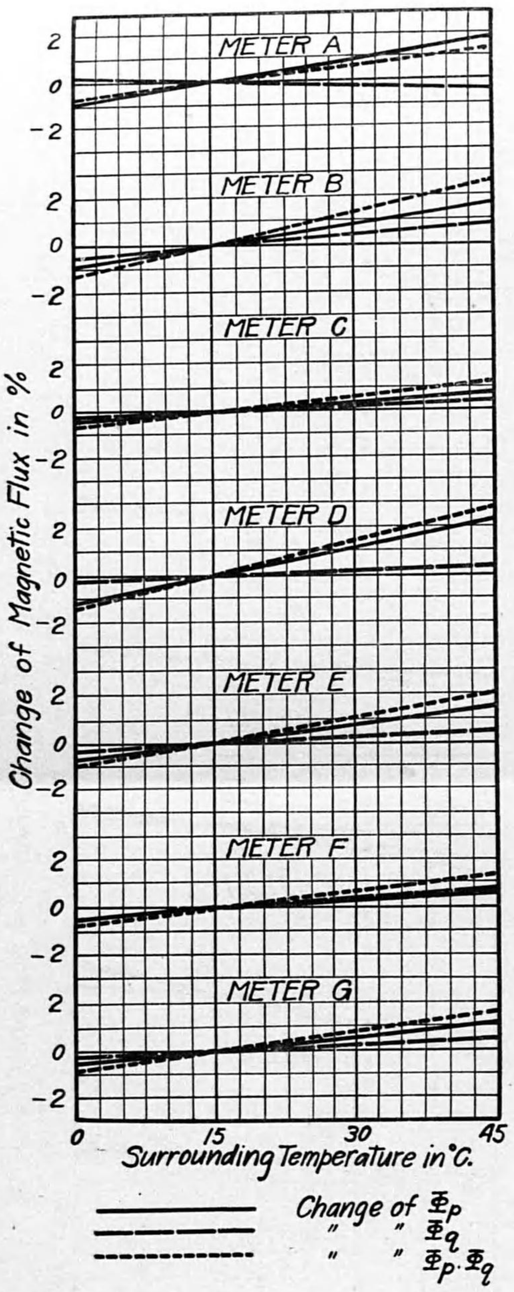
METER A
METER B
METER C
METER D
METER E
METER F
METER G
Change of Magnetic Flux in %
Surrounding Temperature in °C.
0
15
30
45
Change of Φp
" " Φq
" " Φp. Φq

Fig. 31.

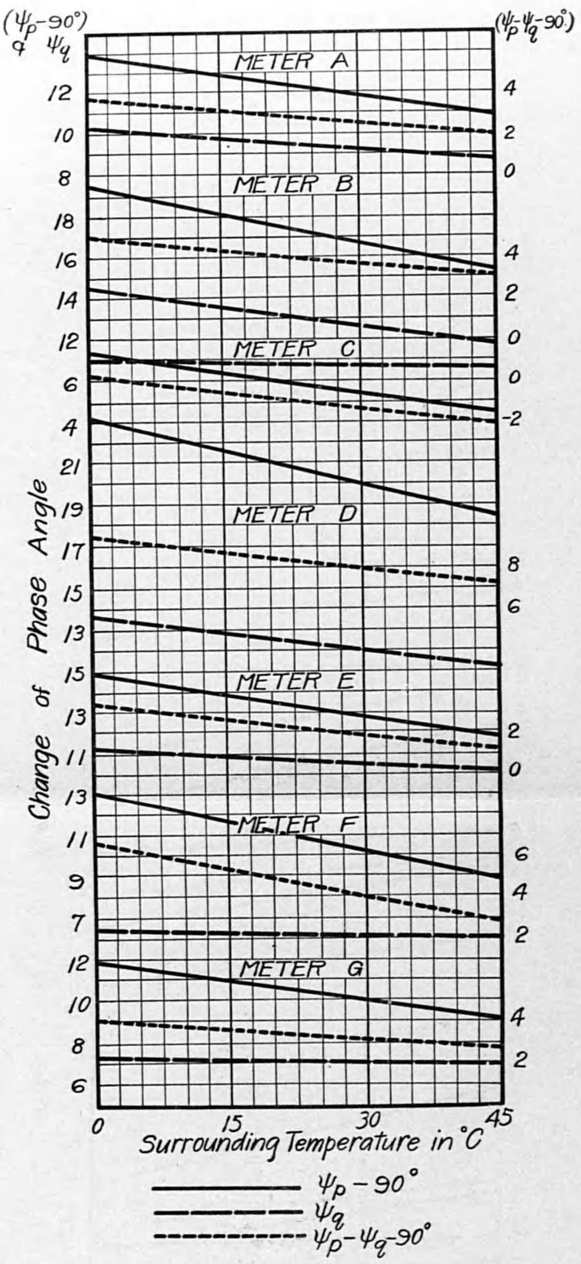
(ψp-90°) of ψq
(ψp-ψq-90°)
METER A
METER B
METER C
METER D
METER E
METER F
METER G
Change of Phase Angle
Surrounding Temperature in °C
0
15
30
45
ψp - 90°
ψq
ψp - ψq - 90°

Fig. 32.

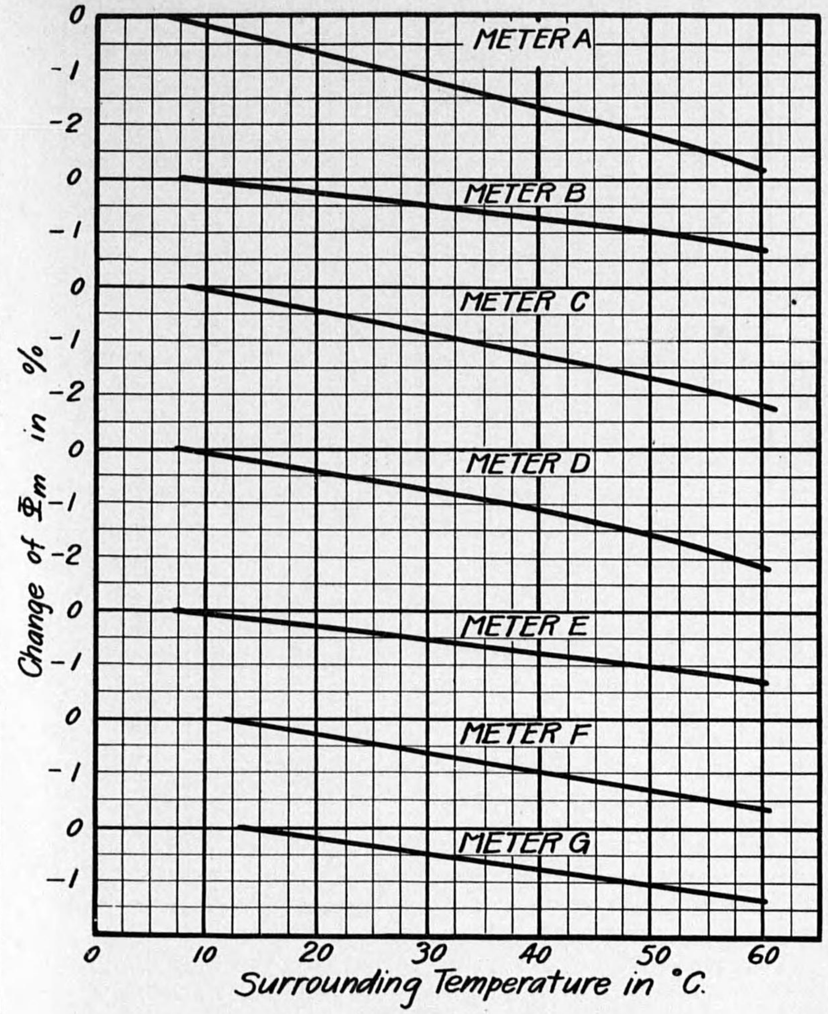
METER A
METER B
METER C
METER D
METER E
METER F
METER G
0
-1
-2
0
-1
0
-1
-2
0
-1
0
-1
0
-1
Change of Em in %
0
10
20
30
40
50
60
Surrounding Temperature in °C.

Fig. 34a

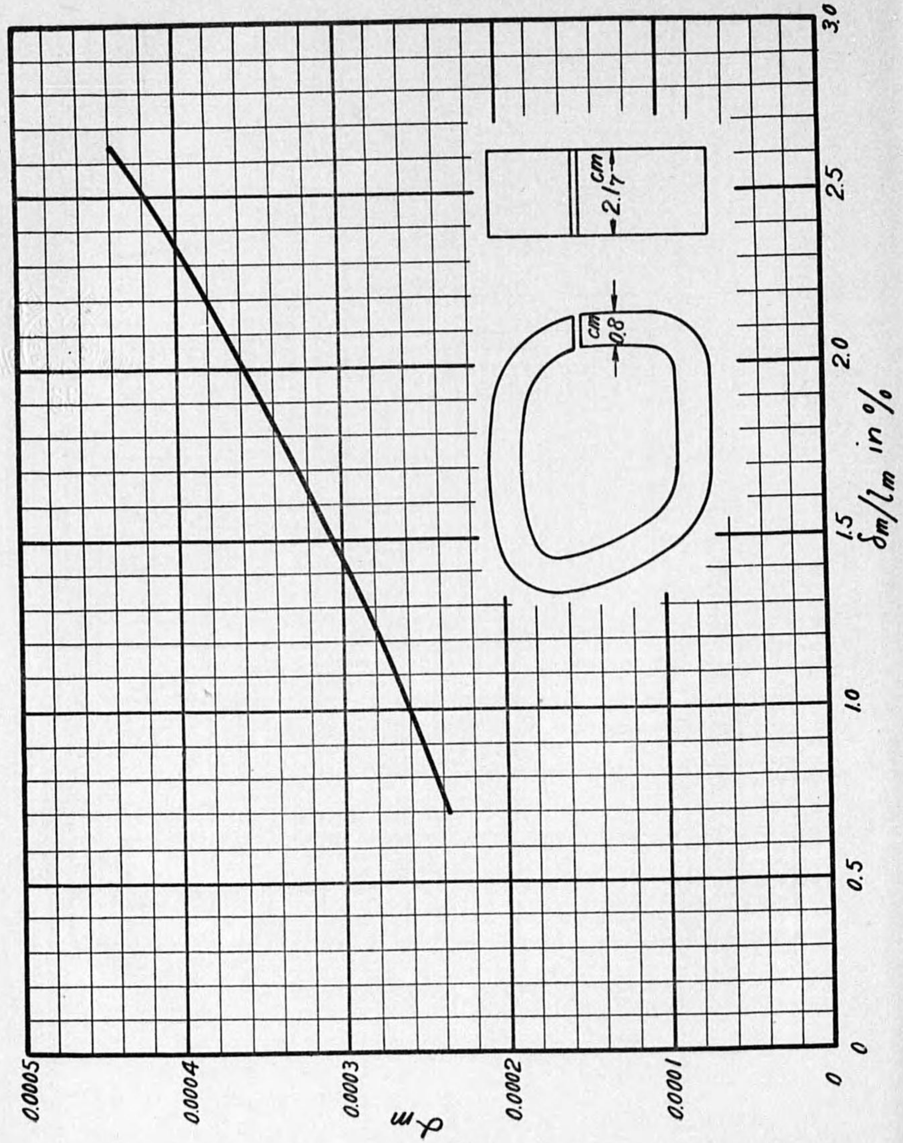

FIG. 34B

TABLE IX.

Meter	α_p	α_q	α_m	Measured Temperature Coefficient	Calculated Temperature Coefficient	β_p	β_q	Measured Temperature Coefficient	Calculated Temperature Coefficient
A	0.06_0%	-0.01_1%	0.05_0%	0.11_1%	0.14_0%	0.11_9%	0.05_5%	0.04_9%	0.06_4%
B	0.06_3	0.03_1	0.02_4	0.14_2	0.14_2	0.16_9	0.10_8	0.08_3	0.06_1
C	0.02_7	0.00_9	0.04_4	0.12_1	0.12_4	0.10_8	0.00_9	0.04_8	0.09_9
D	0.08_2	0.01_1	0.03_4	0.13_1	0.16_1	0.19_2	0.09_6	0.05_0	0.09_6
E	0.05_1	0.01_3	0.02_5	0.10_0	0.11_4	0.11_9	0.03_8	0.05_3	0.08_1
F	0.01_8	0.02_0	0.03_6	0.08_0	0.11_0	0.16_8	0.03_2	0.08_5	0.13_6
G	0.03_5	0.01_7	0.02_9	0.01_1*	0.10_8	0.07_6	0.02_3	0.02_4	0.05_3

* With Temperature Compensating Device.

CHAPTER VIII. PRINCIPLE ON DESIGN OF METER.

1. Characteristic Constant.

The character of meter can be readily adjusted at will, hence the principle of design will stand on the intrinsic character of meter.

Now the author proposes the following characteristic constants which are closely related with the intrinsic character as well as the durability of accuracy,

$$\left.\begin{array}{ll} f_t = \text{Revolutions per second at the rated condition} & \\ C_m = \Psi_d / f_t & \text{in cm gr sec} \\ C_t = \Psi_d / W & \text{in cm} \\ C_p = \Psi_{tp} / \Psi_t & \text{in \%} \\ C_q = \Psi_{tq} / \Psi_t & \text{in \%} \\ C_l = W_l / E & \text{in Watt per Volt} \end{array}\right\} \quad \ldots \quad (71)$$

These numerical values are assembled in Table X. The meanings of these constants are explained as follows,

(**a**) The rated speed of disc f_t will be closely related with the durability of accuracy. When f_t is large, this durability will decrease, owing to the defacement in pivot or ball and the demagnetization in permanent magnet. However, f_t is smaller, the production cost will increase. Usually, f_t will be chosen from 0.5 to 1.0.

(**b**) C_m is a measure of the braking torque. At the double poles type, this constant is remarkably large, but it will not be considered to be economically efficient. If we can obtain the magnet which are always uniform, it will not be difficult to be C_m so large as 6 or 7 at the single pole type.

(**c**) C_t is closely related with the load character as well as the durability of accuracy, because the starting friction is nearly proportional to W and the defacement in pivot or ball is, of course, dependent upon W and f_t. While C_t is greater, the production cost will be greater. Usually C_t will be chosen from 0.2 to 0.4.

(**d**) C_p and C_q are closely related with the voltage character and the load character. These constants are smaller, the characters are better. While, one of

them is smaller, the other is, as necessary consequence, greater. So that it will be reasonable to determine these constants as nearly equal as possible. These constants are usually from 2% to 5%.

(e) The specific power loss in the pressure coil is a measure of power loss in the supplier. Then this constant must be as small as possible. Recently, we will find C_l as small as 0.005.

2. Principle on Design.

The author establishes a principal course of design according to the characteristic constants above mentioned.

Firstly, we will consider of the pressure coil. The specific power loss in this coil can be given by

$$C_l=\frac{E}{r_m N}\psi_{p1}^2$$

Hence, we have

$$N=\frac{E\,\psi_{p1}^2}{r_m C_l} \quad \cdots\cdots\cdots\cdots\cdots\cdots \quad (72)$$

where N denotes the number of turns, r_m the mean resistance per turn and $(\pi/2-\psi_{p1})$ the phase angle between E and the exciting current I_e.

Althogh the magnetic flux Φ_{p1} and Φ_{pm} are not in the same phase with the exciting current, owing to some metallic substances in the main path of pressure flux, we now suppose that those are in same phase, because the above phase deviations are usually very small. Let L be the effective inductance in the pressure coil, L is, of course, proportional to the square of N and inversely proportional to the length of air gap δ_{gm} in the main magnetic path. Putting $q=100\ \Phi_{p1}/\Phi_{pm}$, then we have $\delta_{gm}/\delta_g=q$. δ_g is nearly constant in actual case, then we have

$$\psi_{p1}=R/\omega L=qr_m/k_m f N$$

or

$$q=k_m f N\,\psi_{p1}/r_m \quad \cdots\cdots\cdots\cdots\cdots\cdots \quad (73)$$

where k_m is a constant, of which the mean value is nearly $6.4\cdot10^{-5}$ as shown in Table XII.

On the other hand, we have

$$E=4.44 f N \Phi_{pm} 10^{-8}$$

Therefore we have

$$\Phi_p=14\,E\,\psi_p/r_m \quad \cdots\cdots\cdots\cdots\cdots\cdots \quad (74)$$

$$\Phi_{pm}=100\,\Phi_p/q \quad \cdots\cdots\cdots\cdots\cdots\cdots \quad (75)$$

The phase angle ψ_{p1} in the above equations will be considered as an auxiliary characteristic constant which is closely related with the frequency character.

The frequency error will chiefly result from the change in the phase angle of pressure flux, and the frequency character will be written as

$$\varepsilon_f=\varepsilon_0-\psi_{p2}^2\,\Delta_f$$

where ε_0 denotes the error independent of frequency, ψ_{p2} the phase lag due to the phase compensating device, Δ_f the percentage variation of frequency. On the other hand, we have

$$\psi_{p1}=\psi_{p2}-\psi_q$$

While ψ_q is nearly constant and 0.2 as shown in Table XIII.
Neglecting ε_0, we have

$$\psi_{p1}\leqslant\sqrt{\frac{\varepsilon_f}{\Delta_f}}-0.2 \quad \cdots\cdots\cdots\cdots\cdots\cdots \quad (76)$$

The frequency errors in the standards in various countries[8]-[22] are as follows,

Standard	Δ_f in %	ε_f in %	$\sqrt{\frac{\varepsilon_f}{\Delta_f}}$ in radian
Japanese	5	1	0.45
British	5	1	0.45
U. S. A.	5	1.5	0.55
Swiss	10	3	0.55

Therefore ψ_{p1} must be ordinally less than 0.25 radian.

As already mentioned, we have

$$\left.\begin{aligned} C_p &= k_p \frac{\Phi_p}{\Phi_q} \frac{f_d}{f} \\ C_q &= k_q \frac{\Phi_q}{\Phi_p} \frac{f_d}{f} \end{aligned}\right\} \quad \cdots\cdots\cdots\cdots\cdots (77)$$

Putting

$$\zeta = a/R \qquad \xi = b/R \qquad \eta = d/R$$

where a is the radius of equivalent circle of flux-boundary, b the distance between two adjacent poles, d the distance from the rotating axis to the pole. In actual case, the geometrical constant for driving torque depends on these factors, while the reasonable values of ξ and η are determined by ζ, therefore all geometrical constants depend on ζ only. Now we put

$$k = P/\zeta \quad \text{and} \quad k = Q/\zeta \quad \cdots\cdots\cdots\cdots (78)$$

From these relation, it follows

$$\Phi_q = \Phi_p \sqrt{\frac{PC_q}{QC_p}} \quad \cdots\cdots\cdots\cdots (79)$$

$$\zeta = \frac{f_d}{f} \sqrt{\frac{PQ}{C_p C_q}} \quad \cdots\cdots\cdots\cdots (80)$$

Similarly we can suppose

$$G_d = K/\zeta \quad \cdots\cdots\cdots\cdots (81)$$

On the other hand, we have

$$\left.\begin{aligned} \Psi_d &= f_d C_m \\ c &= \frac{g \Psi_d}{2\sigma f \Phi_p \Phi_q G_d} \end{aligned}\right\} \quad \cdots\cdots\cdots\cdots (82)$$

Let k_w be the ratio of W to the weight of disc itself, k_w is usually about 1.2. Then we have

$$R = \sqrt{\frac{\Psi_d}{\pi k_w m e C_d}} \quad \cdots\cdots\cdots\cdots (83)$$

C_m is known, then the brake magnet can be designed according to the theory in the chapter III. . In this time, it is noticeable that a_m will be considerably large compared with a_c.

Through the above course, the essential parts of meter can be designed. Many data necessary in the design are assembled from Table X to XIV.

3. Numerical Example.

Now we will consider a meter where the magnetic flux are uniformly distributed in a circular boundary. In this case, we can write from the chapters II and III,

$$P = 0.36 \qquad Q = 0.85 \qquad \text{and} \qquad K = 0.38$$

The rated voltage is 100 volts and the marked frequency 50 cycles.
The characteristic constants will be chosen as follows,

$f_d = 1.0$	$C_m = 5.0$ (single pole type)
$C_d = 0.35$	$C_p = C_q = 2\%$
$C_i = 0.005$	$\psi_{pi} = 0.20$ radians

The constants are as follows,

$k_w = 1.2$	$\sigma = 3.4 \cdot 10^{-4}$
$r_m = 0.2$ ohm	$k_m = 6.4 \cdot 10^{-5}$
$m = 2.7$	$g = 980$ (at Tokyo)

According to the equations from (72) to (83), we have

$N=4{,}000$ $\Phi_p=1{,}400$ $q=12.8\%$

$\Phi_{pm}=11{,}000$ $\Phi_q=910$ $\Psi_d=5.4$ cm-gr

$\zeta=0.3$ $G_d=1.3$ $c=0.09$ cm

$R=4.0$ cm

In this case, we can perform the designing in details,

$a=\zeta R=1.2$ cm

$b=\sqrt{2}\ R\zeta=1.7$ cm

$d=(0.9-1.4\,\zeta)\ R=2{,}0$ cm

If the poles are square in which the flux densities are nearly constant, the above data will enable us to roughly estimate the essential part of meter.

TABLE X.

Meter	Rating	Testing Constant	Ψ_d	f_d	C_m	C_d	C_f	C_p	C_q	C_t
		Rev./kwh	cm-gr	r. p. s.	cm-gr-sec.	cm	%	%	%	W/V
A	1-φ, 100V 5 A, 50~	8,000	4.7_8	1.11	4.3_0	0.22	0.31	4.8	5.4	0.005_1
B	1-φ, 100V 5 A, 60~	7,200	4.1_5	1.00	4.1_5	0.21	0.24	5.3	2.9	0.006_8
C	1-φ, 100V 5 A, 60~	5,000	2.8_5	0.69	4.1_5	0.16	0.49	3.2	1.9	0.006_3
D	1-φ, 100V 10A, 50~	3,200	4.7_4	0.89	5.3_0	0.16	0.93	3.6	6.9	0.004_4
E	1-φ, 100V 5 A, 50~	4,320	4.6_6	0.60	7.8_0	0.21	0.34	4.0	2.6	0.004_8
F	1-φ, 100V 5 A, 60~	4,000	3.6_1	0.56	6.4_0	0.22	0.17	2.4	2.2	0.007_5
G	1-φ, 110V 5 A, 60~	1,667	5.3_8	0.25_5	21.0_0	0.40	0.01	2.2	0.8	0.011_2

TABLE XI.

Meter	$2R$	c	W	k_w	Register	Bearing	Ψ_f	I_s / I_f	δ_g	W_t
	cm	cm	gr				cm-gr	%	cm	kgr
A	8.5	0.12	22	1.20	Cyclo	Semi-ball-pivot	0.015	0.6	0.23	1.15
B	7.9	0.13	20	1.16	〃	〃	0.010	0.3	0.22	1.36
C	7.6	0.13	$17._4$	1.10	〃	Pivot	0.014	0.2	0.29	1.12
D	9.5	0.14	30	1.12	〃	〃	0.044	0.5	0.30	1.36
E	8.5	0.12	22	1.20	〃	Ball	0.016	0.3	0.21	1.35
F	8.9	0.08	$16._5$	1.22	Pointer	Pivot	0.006	0.3	0.35	2.34
G	8.9	0.06_7	$13._3$	1.18	〃	〃	0.005	0.5	0.40	3.65

TABLE XII.

Meter	N	I_e	R	r_m	B_{pm}	Φ_{pm}	Φ_p	Ψ_{p1}	q	Ψ_{bp}	W_l	k_m
		mA	ohm	ohm				rad.	%	cm-gr	w	$\times 10^{-5}$
A	6,000	20	1,250	0.20	6,900	6,790	1,570	0.25_4	23	0.22_6	0.51	6.0
B	5,400	22	1,370	0.25	3,900	5,590	1,290	0.31_0	23	0.23_8	0.68	5.7
C	4,700	26	960	0.20	5,100	7,400	730	0.22_7	10	0.09_3	0.63	6.2
D	7,500	14	2,240	0.30	5,000	4,950	1,550	0.31_8	31	0.16_9	0.44	7.8
E	6,000	14	2,290	0.38	4,400	7,360	2,280	0.33_8	31	0.18_9	0.48	11.6
F	4,700	27	1,050	0.22	2,500	6,690	1,180	0.28_5	18	0.08_7	0.75	4.9
G	2,200	93	140	0.06_5	5,700	18,080	3,410	0.12_0	19	0.11_9	1.23	7.8

TABLE XIII.

Meter	AT	B_q	Φ_q	Ψ_q	V	Power Loss	Ψ_{bq}
				rad.	v	w	cm-gr
A	190	670	830	0.14_7	0.48	1.58	0.25_9
B	220	600	620	0.29_1	0.40	1.17	0.11_9
C	100	600	670	0.16_1	0.15	0.59	0.05_5
D	180	820	900	0.19_9	0.19	1.54	0.32_8
E	160	330	760	0.17_4	0.30	0.85	0.12_2
F	145	690	1,030	0.10_3	0.20	0.76	0.07_9
G	80	850	820	0.09_6	0.07	0.19	0.04_2

TABLE XIV.

Meter	Φ	B_m	a_c	b_c	b_c/a_c	$\tilde{c}_m$	l_m	d_m	θ	$\tilde{c}_m/c$	$\tilde{c}_m/l$	d_m/R
			cm	cm		cm	cm	cm	°		%	%
A	6,770	4,800	0.63	2.23	3.54	0.22	13.9	2.6	5	1.83	1.6	61
B	7,090	5,000	0.63	2.25	3.56	0.24	13.5	2.6	30	1.84	1.8	61
C	6,780	4,300	0.70	2.25	3.20	0.23	12.2	2.0	7	1.78	1.9	53
D	6,120	4,000	0.62	2.47	3.95	0.25	15.6	2.7	20	1.88	1.6	57
E	8,370	4,450	0.71	2.64	3.70	0.23	13.4	3.4	0	1.92	1.7	80
F	7,570	4,050	0.82	2.28	2.78	0.23	18.5	2.9	25	2.88	1.25	65
G	7,190	3,800	0.91	2.10	2.30	0.21	15.2	2.8	20	3.14	1.4	63

CHAPTER IX. SUMMARY.

In this paper, it is intended to offer the materials necessary in the design of induction watthour meter.

The important articles in this paper are summarized as follows.

1. The author proposes **Geometrical Constant** which has the important meanings on the design as well as the criticism of meter.

2. The theoretical study is performed from the following assumptions,

(a) the magnetic flux are uniformly distributed in a circle and the phase angles of flux are everywhere constant within the circle.

(b) the linear velocity of disc is constant within the flux-boundary; in other words, the flux-boundary is very small compared with the disc. (for the case of retarding torque)

3. The geometrical constant of driving torque can be generally represented by the ratio of the perpendicular distance from the rotating axis to the line through two centres of circles to the distance between these centres, where the circles do not intersect.

4. The geometrical constant, where the circles intersect, can be obtained, and the complete equation in practical case is given.

5. The simple relation between this constant and the relative dimension of circle respecting to disc is explained.

6. The geometrical constant of retarding torque due to single pole can be generally represented by the square of the ratio of the distance from the rotating axis to the centre of circle to the radius of circle.

7. The geometrical constant of retarding torque between two poles can be generally represented by $r_p r_q/r^2 \cos(a_p+a_q)$, where r_p, r_q are the distances from the rotating axis to the centres of circles, r the distance between these centres, a_p, a_q the angles between r and r_p or r_q measured in same direction from the line r.

8. The geometrical constant of braking torque is approximately deduced.

9. The flux distributions are investigated on various meters, and the magnetic reaction due to eddy current is resolved experimentally.

10. The finished meters are criticized according to the geometrical constants and the configuration of flux-distribution.

11. A precise method of measuring the retarding torque is proposed.

12. The relation between the frictional torque and the weight of moving part is invesligated, and it is pointed out that the semi ball pivot bearing will be most recommended.

13. The theoretial results are ascertained by the experiment on a meter especially made, with respect to driving torque and retarding torque.

14. A complete equation of load character is proposed and the methods of improving this character are pointed out.

15. The load character is experimentally analized on various meters.

16. A complete equation of temperature character is proposed and the methods of improving this character are pointed out.

17. The temperature character is experimentally analized on various meters.

18. A precise method of measuring temperature coefficient of permanent magnet is proposed and the relation between this coefficient and the ratio of air gap to the length on magnet is cleared up.

19. The author proposes **Characteristic Constant** and the meanings are explained.

20. The principal course of design standing on these characteristic constants is proposed with a numerical example. Many valuable data necessary in the design are tabulated.

The author wishes to thank Messrs. T. Nakao, K. Suda and K. Inagaki for their splendid assistance in carrying out this research.

APPENDIX I.

GEOMETRICAL CONSTANT AT A SPECIAL CASE.

In the case as shown in Fig. 35, the driving torque can be represented by

$$\Psi_d = 2\sigma cf \Phi_p \Phi_q \sin(\psi_p - \psi_q) K_d$$

where

$$K_d = \frac{d}{12\pi a^4} \int_{-\frac{\pi}{2}}^{\frac{\pi}{2}} r_\theta^3 \cos\theta \, d\theta = d/4a$$

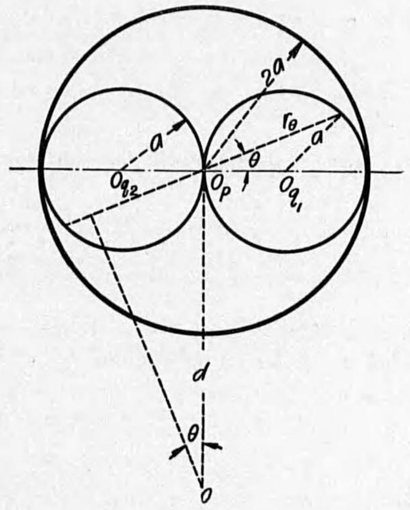

Fig. 35.

In the case of disc, we have

$$T_d = 2\sigma\, cf\, \Phi_p\, \Phi_q \sin(\psi_p - \psi_q)\, G_d$$

where

$$G_d = \frac{\eta}{\zeta}\left\{\frac{1}{4} - \frac{\zeta^2}{(1-\eta^2)^2+\zeta^2\eta^2}\right\}$$

The relation between G_d and ζ, η are shown in Table XV, and from these results we know that the geometrical constants in this case are generally small compared with that in the chapter II.

TABLE XV.

G_d

η \ ζ	0.05	0.10	0.15	0.20
0.4	1.97	0.944	0.582	0.388
0.5	2.46	1.16	0.701	0.450
0.6	2.93	1.36	0.784	0.467
0.7	3.37	1.49	0.719	0.375
0.8	3.70	1.41	0.500	—
0.9	3.32	—	—	—

APPENDIX II.

LITERATURES.

1. W. Rogowski:—Ueber die Vorgange in der Scheibe eines Wechselstrommotorzaehler. (E. u. M. S. 915, 1911)
2. W. Rogowski:—Ueber die induzierte Stromung und das Drehmoment bei der Scheibe eines Wechselstrommotorzaehler. (Archiv. S. 205, 1913)
3. T. T. Fitch and C. J. Huber:—A comparative study of American direct current watthour meters. (B. O. S. Vol. 10, 1913)
4. S. Jimbo and K. Matsumoto: Study on the design of integrating watt meters. (Researches of E. T. L. No. 91, 1921)
5. T. Otake and S. Kato:—Theory of integrating watt meters. (Denki-gakkai. January, 1924)
6. S. Jimbo:—Further study on the induction type watthour meter. (Researches of E. T. L. No. 119, 1924)
7. H. Schering und R. Schmidt:—Der Winkelfehler bei Induktionzaehlern. (Archiv. S. 511, 1923)
8. T. Otake and S. Kato:—Theory of integrating watt meters. (Denki-gakkai. November, 1925)
9. I. F. Kinnard and H. T. Fans:—Temperature errors in induction watthour meters. (A. I. E. E. p. 241, 1925)
10. R. M. Fichter:—Contribution à l'étude des compteurs d'électricité. (Rev. Gén. de L'el. p. 1035, 1083, 1131, 1924)
11. K. Bauer:—Scheiben-strome in Wechselstromfehlern. (Archiv. S. 58, 1926)
12. R. Schachenmeiner:—Beitrag zur Theorie des Spannungssystems von Induktionmessgeraten. (Archiv. S. 178, 1926)
13. A. R. Knight and M. A. Faucett:—Effect of temperature on single phase induction watthour meters. (Univ. Illinois. p. 153, 1926)

14. T. Spooner:—Temperature coefficient of magnetic permeability of sheet steel. (Phy. Rev. p. 183, 1926)

15. F. Bergtold:—Untersuchungen am Ferrariszaehler. (Archiv. S. 373, 1926)

16. D. T. Caufield:—Theory of action of the induction watthour meter and analysis of its temperature errors. (A. I. E. E. p. 328, 1927)

17. S. Jimbo and T. Nakao:—On the method of measurement of retarding torque in watthour meter. (Dai-ichibu-iho of E. T. L. Vol. 2, No. 2, 1927)

18. Standard specification of watthour meter. (Japanese Electrotechnical Committee, 1926)

19. British Standard Specification for Electricity Meter. (1919)

20. Code for Electricity meters. (proposed revision, 1927)

21. Bestimmungen fur die Beglaubigung von Elektrizitatzaehlern. (1921)

22. Vollziehungs verordnung betreffend die amtliche Prufung und Stempelung von Elektrizitats-verbrauchsmesserm. (1922)

23. European meters. (Serial report of N. E. L. A. November, 1926)

24. Report for the year 1927. (N. P. L. p. 165, 1928)

25. S. Jimbo and T. Nakao: On the induction watthour meters. (Denki-gakkai. March, 1928)

昭和3年10月13日印刷
昭和3年10月16日發行

電氣試驗所編

發行・印刷人
倉橋藤治郎
東京市麹町區有樂町1工政會

發行所
工政會出版部
東京市麹町區有樂町1—1
電話丸の内(23)3980番
4647番
振替東京27724番

¥2.20

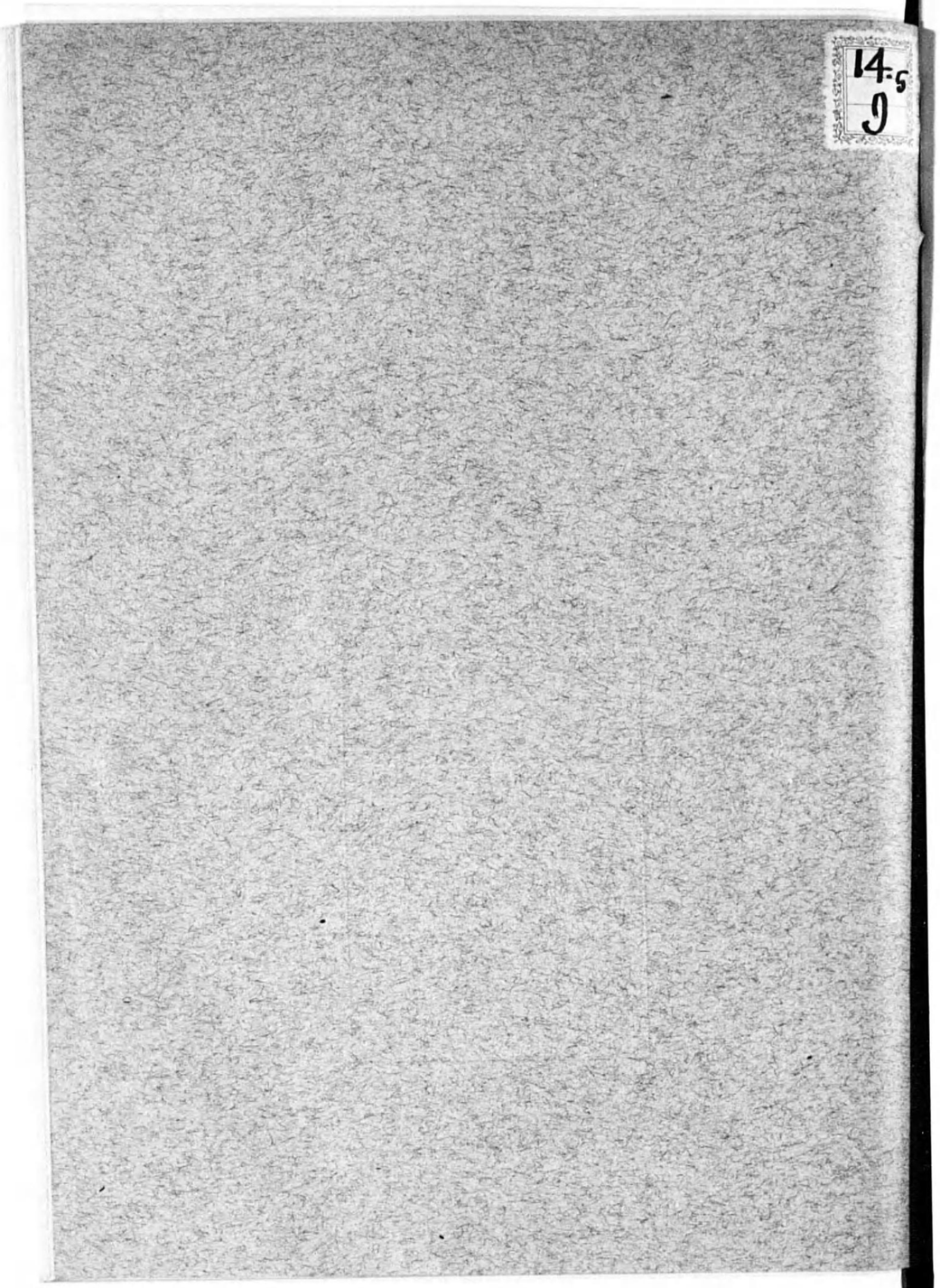

終